

AD/A-002 218

HEAT TRANSFER DESIGN AND PROOF TESTS
OF A RADIOISOTOPE THERMOELECTRIC
GENERATOR

Earl J. Beck

Civil Engineering Laboratory (Navy)

Prepared for:

Naval Facilities Engineering Command

November 1974

DISTRIBUTED BY:

NTIS

National Technical Information Service
U. S. DEPARTMENT OF COMMERCE

Unclassified

SECURITY CLASSIFICATION OF THIS PAGE (When Data Entered)

REPORT DOCUMENTATION PAGE		READ INSTRUCTIONS BEFORE COMPLETING FORM	
1 REPORT NUMBER TN-1359	2 GOVT ACCESSION NO.	3 RECIPIENT'S CATALOG NUMBER AD/A-002218	
4 TITLE (and Subtitle) HEAT TRANSFER DESIGN AND PROOF TESTS OF A RADIOISOTOPE THERMOELECTRIC GENERATOR		5 TYPE OF REPORT & PERIOD COVERED Final; Nov 1972-Jul 1974	6 PERFORMING ORG REPORT NUMBER
		8 CONTRACT OR GRANT NUMBER(s)	
7 AUTHOR(s) Earl J. Beck		9 PERFORMING ORGANIZATION NAME AND ADDRESS CIVIL ENGINEERING LABORATORY Naval Construction Battalion Center Port Hueneme, CA 93043	
11 CONTROLLING OFFICE NAME AND ADDRESS Naval Facilities Engineering Command Alexandria, VA 22332		10 PROGRAM ELEMENT PROJECT, TASK AREA & WORK UNIT NUMBERS 63724N, Y41W1, 43-016.	12 REPORT DATE November 1974
14 MONITORING AGENCY NAME & ADDRESS (if different from Controlling Office)		13 NUMBER OF PAGES 51	15 SECURITY CLASS (of this report) Unclassified
		15A DECLASSIFICATION/DOWNGRADING SCHEDULE	
16 DISTRIBUTION STATEMENT (of this Report) Approved for public release; distribution unlimited.			
17 DISTRIBUTION STATEMENT (of the abstract entered in Block 20, if different from Report)			
18 SUPPLEMENTARY NOTES			
19 KEY WORDS (Continue on reverse side if necessary and identify by block number) Thermoelectric generator, RTG, radioisotope powered, electrical power, underwater power, heat transfer, natural convection, under-ocean heat rejection surface			
20 ABSTRACT (Continue on reverse side if necessary and identify by block number) In support of a larger effort of the Nuclear Division, Naval Facilities Engineering Command, CEL undertook to design, build, and test the heat rejection portions of a large 2-kw(e) radioisotope thermoelectric generator (RTG). The design was optimized to produce the lowest practicable temperatures at the cold junction of a large number of thermoelectric heat-to-electricity conversion elements. The geometry was largely defined continued			

DD FORM 1473 EDITION OF 1 NOV 65 IS OBSOLETE

Unclassified

SECURITY CLASSIFICATION OF THIS PAGE (When Data Entered)

Reproduced by
NATIONAL TECHNICAL
INFORMATION SERVICE
US Department of Commerce
Springfield, VA 22151

Unclassified

SECURITY CLASSIFICATION OF THIS PAGE (When Data Entered)

20. Continued

by the size, shape, and required number of thermoelectric elements and by their deployment at the upper end of a large pressure-resistant hull. The work showed the capability of the 12-finned convectors to maintain a temperature below 90°F at the inner face of the convectors both when the unit was vertical and when tilted 60 degrees from the vertical. The solid copper showed no signs of corrosion; the potential corrosion problem is discussed in some detail in the report, as are related problems of flow, protection, and possible fouling from marine growth.

Unclassified

SECURITY CLASSIFICATION OF THIS PAGE (When Data Entered)

INTRODUCTION

As one of several activities supporting the Nuclear Division of the Naval Facilities Engineering Command in developing a large 2-kw(e) undersea radioisotope thermoelectric generator, the Civil Engineering Laboratory undertook in late 1972 the design optimization, construction, and testing of the necessary heat rejection modules.

All known methods of converting heat to electric power inherently must reject a certain amount of the available heat to the environment. Because of their relatively low efficiency, thermoelectric generating elements reject a relatively large amount of heat, some 28 to 30 kw for a 2-kw(e) unit. The cold waters of the deep ocean are excellent for receiving heat, and the potential exists for attaining a near-maximum efficiency by keeping the cold junction of the thermoelectric conversion units as near the ambient ocean temperature as is practicable. The colder the cold junction, the better the efficiency and, probably, the life of the elements.

The practical foundation for convection heat transfer, entirely adequate for the planned use here, is well laid in extensive theoretical and empirical work in the open literature. This work was specialized and extended for the ocean applications in a comprehensive study conducted by and for the Civil Engineering Laboratory by Braun in 1965.* This study included resolution of former discrepancies in published works and extended the resulting correlations to a design method and tests in shallow and deep water in the ocean off Southern California. This work so completely summarizes previous efforts that it is the only reference to be used here. It is far too comprehensive to be abstracted, so its results will be used directly with a minimum of discussion; they relate to design, corrosion, and marine fouling of heat transfer surfaces as well as consideration of the probable height of a heated plume over a natural convector.

Certain assumptions are made by Braun, page II-25 "Optimum Fin Geometry in Free Convection," some of which, while appropriate for industrial heat transfer devices, were not all appropriate in this application.

- Assumption: 1. Steady-state heat flow. Valid, and realistic in the ocean.
- Assumption: 2. Homogeneous fin material and constant fin thermal conductivity. Valid, at least for the first trial designs. The possibility of incorporating ducting (heat pipe type passages) within the fins may be considered later, which would invalidate this assumption.

* C. F. Braun Co., Alhambra, CA. "Study of heat transfer and fouling of heat transfer surfaces in the deep ocean-final report," Contract NB 32274, 26 November 1965.

- Assumption: 3. Constant heat transfer coefficient over the face of the fin. Not valid, but a useful first approximation in developing a fin cross section using the technique of an analog computer based on resistive paper.
- Assumption: 4. Uniform temperature in the surrounding fluid. Obviously not strictly valid, but a useful approximation as in Assumption 3.
- Assumption: 5. No temperature gradients occur along the length and across the thickness of the fin. Invalid, but approximately correct for very high conductivity in the fins (copper, silver, etc.) and low surface coefficient.
- Assumption: 6. Temperature at the fin base is uniform, and there is no contact resistance at the fin base. Valid, first part approximately correct for high-conductivity materials such as copper; second part valid for most construction methods, including brazing, casting, and soldering.
- Assumption: 7. There is no heat source within the fin itself. Valid for solid fins. With internal ducting, as with heat pipe channels, not valid.
- Assumption: 8. Heat transfer from the fin end and sides is negligible. Valid for all but thickest and shortest (in direction of water flow) fins.

The usual industrial criterion for heat transfer surface optimization is cost, and the methods outlined in the reference are based on cost considerations. For the present design, the relatively low cost of the heat rejection surfaces no matter how constructed appeared trivial compared to the probable costs of the remainder of the RTG design. Therefore, a design method based on the following criteria was adopted:

(a) Within the physical constraints of size based on the number and size of the pre-existing thermoelectric units, provide a minimum base temperature at the cold junction of the thermoelectric units.

(b) Provide as uniform a base temperature as practicable, which means a fairly heavy section of high-conductivity material.

(c) Provide the necessary strength in longitudinal compression for the intended overpressures. The thermoelectric units are fabricated by an intense swagging process and can provide the necessary strength in the radial direction.

(d) Provide a maximum of protection against corrosion.

(e) Provide a maximum of protection against marine growth.

(f) Fabricate by a method that will insure optimum quality control. For the immediate demonstration experiment, fabricate to as nearly the final design as practicable by a low-cost method.

The remainder of this report describes the design methods, the final design selected, the results of controlled tests in a large tank of seawater at CEL, and the results of a 30-day immersion in Port Hueneme Harbor.

DESIGN AND OPTIMIZATION OF THE HEAT TRANSFER MODULES

Previous criteria provided by the sponsor, required that some 28 kw of heat be rejected in 12 vertical modules of the overall dimensions shown in Figure 1. All of the useful heat to be converted in part to electricity must be transferred radially from a high temperature heat pipe in an area as shown. To provide for compression strength in the longitudinal direction, at least 3/16 inch of most copper alloys would be required, not crediting the additional strength and rigidity provided by any fins used in the final design. A thimble thickness of 1/4 inch was arbitrarily selected to utilize readily available materials. Based on a design overpressure of 10,000 psi (approximately equivalent to a 20,000-foot immersion depth in seawater), the resulting longitudinal compressive stress in the 1/4-inch-thick thimble is:

$$S_c = \frac{\pi(D^2/4)P}{\pi(D^2 - d^2)/4} = \frac{D^2 P}{D^2 - d^2} = 16,500 \text{ psi*} \quad (1)$$

for the dimensions shown in Figures 2 and 3, or about 1/6th the probable compressive strength for structural copper; stronger alloys would provide an even greater margin, as would any heavy fins--an almost certain eventuality in this type of convector. The heavy section is desirable to produce even temperatures at the minor diameter, d, and a long life in the presence of corrosion.

Seawater is an excellent cooling medium; however, for the relatively high unit area heat loading of 2,600 watts on a 0.308-square-foot base area,

$$Q/A = \frac{(2600)(3.4)}{0.308} = 28,700 \text{ Btu/(hr)/(ft}^2\text{)}$$

an extended surface consisting of a number of vertical, heavy fins will almost certainly be needed to produce a low base temperature.

As a first trial, the following calculation was made of the temperature drop through 70-30 copper-nickel:

* See List of Symbols after Appendix B.

$$Q = \frac{-K A \Delta t}{x}; \quad \Delta t = \frac{x Q}{-K A} = \frac{(0.25)(8,850)}{(200)(0.378)}, \quad \text{or } 29.6^{\circ}\text{F} \quad (2)$$

for a 1/4-inch-thick thimble. While not unreasonably high, it would produce base temperatures well over 100°F with natural convection heat transfer to 40°F seawater. Much better results would be obtained with copper. For the Cu-Ni case, the temperature drop from the base would be approximately as shown schematically in Figure 2. This figure also shows a first estimate of the full-scale cross section of idealized heavy fins. The final shape and height, H, selected were eventually modified to reduce manufacturing costs and to avoid interlocking of the fins of adjacent modules on the prescribed base circle (21.25 inches diameter) for the 12 modules. The results are slightly nonconservative compared with the ideal shape (Figure 2) with ample fillets at the base and parabolic cross section. That is, the more expensive, longer fins would provide slightly better cooling; the difference is marginal.

The bare thimbles would have a base temperature well over 200°F, which would be undesirably high. An extended surface (fins) to produce additional heat transfer area is clearly indicated. Because of the high heat loading, the optimum fins will require: (a) heavy cross section, to avoid excessive temperature drop along their length, (b) a material of high thermal conductivity for the same reason, and (c) as close spacing as practical without reducing flow to the base.

The actual value of the film coefficient, h, is determined by the well-known dimensionless equation as refined by Braun (1965) for seawater:

$$\text{Nu} = f(\text{Pr}) (\text{Ra})^n \quad (3)$$

in which f is an experimental constant and the exponent n is typically 1/4 up to Grashoff's number of about 10⁹, and 1/3 above 10⁹. The lower value is associated with laminar flow, the higher value with turbulence.

For the fin length, L, dictated by the design and the physical properties of seawater at pressures equivalent to 20,000-foot depth:

$$c_p = 0.95 \text{ Btu}/(\text{lb})(^{\circ}\text{F})$$

$$\rho = 64 \text{ lb}/\text{ft}^3$$

$$\mu = 1.66 \text{ lb}/(\text{ft})(\text{hr})$$

$$K = 0.385 \text{ Btu}/(\text{hr})(\text{ft}^2)(^{\circ}\text{F}/\text{ft})$$

$$\beta = 1.15 \times 10^{-4}/^{\circ}\text{F}$$

$$L = 0.5 \text{ ft}$$

$$g = 4.17 \times 100 \text{ ft}/(\text{hr})(\text{hr})$$

$$\text{Pr} = c_p \mu / K = 5.68 \text{ (dimensionless); at 1 atmosphere, this is about 4.5}$$

While the design is for the deep ocean, say 20,000 feet, the immediate results must be related to 1 atmosphere; comparable values of the important physical properties and resulting dimensionless numbers are tabulated in Table 1. Because of the small change in physical properties in the direction of improved heat transfer with depth, results from the 1-atmosphere tests are slightly conservative--metal surface temperatures will be slightly lower in the actual deep-ocean applications. The $f(Pr)$ is shown as a function of Pr , Figure 3, and the values for the shallow and deep water indicated in the curve. For the remainder of the report, shallow water values only will be used.

OPTIMIZATION OF EXTENDED SURFACES--ITERATIVE APPROACH

Referring to Equation 1 and Figure 1, it is obvious that the only physical aspect of the heat rejection surface related to h is the height, L , which is fixed by the dimensions of the thermoelectric elements to be used. The other important parameters are the physical properties of the fluid, the temperature difference (Δt), and the exponent--which is assumed to be $1/4$, as the Grashoff's number is about 10^9 , the approximate upper limit for laminar flow (Braun, 1965). Table 2 gives some estimates of the effect of varying the surface temperature on the convection film coefficient, h , the resulting heat rejection of a bare cylinder, and the increase in area per each of the 12 modules necessary to reject the design value of 8,850 Btu per hour per module.

Because all of the heat transferred from the base area through the extended fin surface must be moved through the fin metal with a loss in temperature proportional to the fin conductivity, there is an obvious tradeoff between long, slender fins (dimension H , Figure 2) to obtain a maximum usable area and short, stubby fins to produce a high surface temperature (minimize temperature drop) and a resulting high convection coefficient, h . Because the heat transferred is proportional to the area and to h , and because h varies as the $1/4$ th power of the temperature difference, there is no simple linear relationship allowing a direct approach to establishing proportions. Using criteria listed earlier, a first design of a possible shape is shown, Figure 4. This stubby fin has approximately 2.5 times the area of the base cylinder and from Figures 5, 6, and 7, this fin should have a surface temperature of about 130°F when transferring the necessary heat to 40°F seawater at low pressures, if made of copper.

A similar, much longer fin made of aluminum ($K = 1,500$, Table 3) would have temperatures approximately as shown in Figure 8. This is the first result of the use of an analog computer which utilizes a high resistance paper to simulate heat conduction and a millivolt meter to read voltages, which simulate temperature. In Figure 8, the surface was divided into ten segments and the surface temperature estimated for each. The method is very rapid and powerful, in that simple shapes can be rapidly produced, and substitution of various fin materials can

be made by varying the current to achieve the desired voltage drop across the base 1/4 inch. At the design heat load, a copper cylinder 1/4 inch thick has a Δt of about 2°F. All other potentially useful materials are of lower conductivity, so they will have a greater temperature drop; for aluminum, this is 3.6°F.

The actual resistance paper used for these and most later iterations is shown in Figure 9, and includes not only the field with pricked points at the grid intersections, but a varying resistance area allowing simulation of the resistance provided by the film coefficient, h . By biasing the outer border to 40°F with an external electrical resistance it is possible to obtain direct voltage readings at any point on the surface which are equivalent to the temperature. Figure 10 shows the same cross section, with temperatures plotted for a first single module designed to provide a prototype for the full-scale 12-module system, shown in Figure 11. This single module is shown schematically in Figure 12 in partial section full size, and in elevation 1/4th size, with some details of its construction. Its method of construction allowed two desirable features: a complex, 'ideal' shape at low cost, and a copper sheath to which could be directly attached a single constantan wire forming a thermocouple junction by which precise surface temperatures could be obtained. The succession of steps followed in checking the design was:

(a) Prepare, bias, and take readings of a preliminary resistance paper half section, four times full size.

(b) Build the prototype, lead-filled single module and equip with electric heaters and a heat transfer liquid consisting of approximately two parts water and one part ethyl alcohol, enough to cover the electric heaters while in the vertical position.

(c) Test the lead-filled prototype in a small tank at two temperatures of water--one at about 70°F, ambient for the Port Hueneme area, and one at about 40°F, using ice water.

(d) Repeat the ambient water tests with the module tilted 30 and 60 degrees from the vertical (a small trunnion was used to maintain stability).

(e) Fill in the field of temperatures, using an electrical bias to reproduce the measured values. Figures 10(a) and 10(b) show the section temperatures at mid-elevation; the temperatures underlined are measured.

The values obtained are recorded in Tables 4 and 5. There was no indication of local overheating or insufficient cooling in any of these first tests.

FULL-SCALE PROTOTYPE EXPERIMENT

Following successful verification of the design to this point using the single lead-filled module (which for purposes of this report is not considered to be a valid experiment, but a design device), 12 full-scale modules made of solid copper were fabricated (Figure 13). Details of fabrication are shown in Figure 14. In effect, each of the 12 copper modules is a small boiler or upper terminus of a heat pipe heated by three electrical immersion heaters of 1,000 watts nominal rating each.

To allow the use of fins of copper, the best material, and at the same time allow fabrication at reasonable cost, stubby rectangular fins were used. Further, this was necessary to avoid interlocking of the fins on the tight circle prescribed by the design; the loss of the extra area had negligible effect on the base temperatures as will be shown later. When the complete RTG is built, there may be a small advantage in using the complex, higher fins--that is, longer in the radial direction, Figure 2. This would require either interlocking the fins or increasing the diameter of the major circle on which the 12 modules are mounted. A close-up view of the copper heat rejection modules is shown in Figure 15, and an underwater view of the completed experiment with instrumentation as tested in CEL's 60,000-gallon tank of seawater in Figure 16.

All temperatures were read from a manually balanced, direct reading portable Leeds and Northrop potentiometer, with a rapid-response electronic null meter. The calibration allowed reading to within $1/2^{\circ}\text{F}$, and estimating somewhat more closely. Thermocouple locations are shown in Figure 17.

Tests of the full-scale device, Figures 11 and 16, were conducted in ambient temperature water in the vertical position as shown and at 30 and 60 degrees from the vertical, without and with a protective shroud which mounted in the four $1/2$ -inch holes which can be seen adjacent to the modules, Figure 13.

The very large volume of water in the tank made it impracticable to reduce the ambient water temperature appreciably with ice without incurring excessive cost and reducing the salinity. One loading of ice was used, and the data are identified in the tabulation of results. The freshwater tended to stratify on the surface as the ice melted because of its lack of salinity. An effort was made to stir the water in the tank, with uncertain results. The normal temperature gradient in the tank from top to bottom was measured at about 2°F .

The only irregularity in experimental procedure occurred when the complete experiment was left in the seawater test tank over a weekend. The single-module lead-filled prototype had as a precaution been vented to avoid pressure build-up in the event of insufficient heat transfer. Provision was made for venting on the full-scale experiment, but the holes were plugged as a simplification, inasmuch as no pressure build-up had been observed in the first prototype. Apparently a faulty O-ring sealing the water-alcohol mixture allowed leakage past the heater elements

in five of the 12 modules. This was observed as an excess electrical load and, while none of the heating elements burned out, they were replaced with new units, and precautionary venting was provided. None of the data included in this report are of tests with defective wet insulation in the heating elements.

DISCUSSION OF RESULTS

The entire point of the experiment was to validate the capability of the module design to dissipate the required heat, measured electrically, and to provide low temperatures at the locations of thermocouples M1, M2, and M3 which are on the surface where they would be in intimate contact with the cold junctions of the thermoelectric units in the actual RTG. The results are tabulated in Tables 1 through 8. A run consisted of adjusting the electrical input to the desired value and observing temperature rise until the inner temperatures were stabilized. Because of the rapid cooling of the seawater, the high thermal diffusivity of the copper fins, and the small mass of the water-alcohol mixture contained in the heat pipes, temperature stability was typically achieved in about an hour from cold start-up and even more rapidly with minor adjustments in power input. To insure stability, a typical run consisted of a 1-1/2 to 2-hour stabilization period, followed by taking a single set of readings.

With the exception of failure of the O-rings containing the alcohol-water mixture as discussed above, there were no observed irregularities nor unexpected temperature anomalies.

While the nominal required heat input to the 12-module experiment was 28 kw total, some tests are for a higher power dissipation, 32 kw. This is slightly over the design heat load, so that the maximum temperatures recorded are somewhat higher than the values which might be expected in a newly fueled RTG deployed in deep-ocean water at, say, 40°F ambient seawater temperature. The temperatures as recorded in the tank tests are shown in Tables 4 and 5.

An appreciation for the linearity of the metal temperature changes with change in ambient seawater can be obtained from Table 6, which gives both the temperatures of the lead-filled single module at two water temperatures, and the differences. With a difference in water temperatures of 35°F, no measured temperature differences greater than 48°F were observed. The most important single temperature, because it is physically closest to the base, is T6. For this location, dropping the water temperature by 35°F caused a metal temperature drop of 43°F, a conservative development in assessing the eventual consequence of immersing a full-scale RTG in very cold, deep-ocean water.

Summarizing the results shown in Tables 7 and 8, there was no evidence under any of the conditions of test of poor flow to and around the modules which cause excessive temperatures or poor cooling. The effect on the inside metal temperatures, those seen by the thermo-electric modules, of

tilting the experiment from the vertical is shown in Figure 18(a). Also shown are the effects on these critical metal temperatures of shrouding the modules with a vertical steel chimney in what might be expected to be the worst case; when the experiment is tilted 60 degrees from the vertical. There was some increase in temperature at all three points of measurement, but no great change which would predict difficulty--the presence of the shroud merely impeded the vertical flow of water in this partially prone position. The effects are, in fact, similar to placing the shroud on the unit when in the vertical position, Figure 18(b). Here, there was some indication of reduced flow to the lower parts of the modules, but essentially no effect at the top, T1. The small decrease in temperature of T1 with the shroud added can be almost exactly accounted for by slightly lower water temperatures.

The efficacy of a shroud is almost universally assumed, because of the apparent 'chimney' effect that might be gained. However, a convector has one major difference from a chimney. In a typical chimney used to produce draft in a furnace, all of the heat is introduced below the chimney, and the draft produced arises from the difference in density between the heated stack gases and the surrounding cool air. There is, of course, a stack effect with the shrouded convector. However, there is what appears to be a more important second effect common to plumes. Without the shroud, cold fluid (water in this case) can be continually entrained--the higher metal surfaces do not see the warmed water, but rather cold water drawn in by the vertical convection current.

Our consideration of the use of a shroud for this application arose not from a desire to enhance the flow and produce marginally lower metal temperatures, but to provide protection for the convection modules from cables, etc, as will be necessary in the ocean. Its usefulness in this function may well justify the small loss in cooling effect caused by the inhibition of inflowing cold water. A schematic of a shroud as it might be utilized on a large RTG is shown in Figure 19.

In assessing the foregoing, it should be remembered that with the cold water typical of the deep ocean (36 to 40°F), all of the metal temperatures would be reduced in proportion. Critical metal temperatures of the order to 70°F or lower would be expected.

A discussion of metal selection based on heat transfer, fouling, and corrosion considerations is contained in Appendix A.

The results of a 30-day immersion in Port Hueneme Harbor at nominal full power are discussed in Appendix B.

It should be noted here that in neither the Laboratory tank tests nor those in the harbor was bare copper exposed, as would be expected with high velocities. The use of copper is satisfactory on that basis.

CONCLUSIONS

1. The design utilizing solid, heavy, short fins on the 12 modules should produce cold junction temperatures in the actual RTG of 70°F or lower in the deep-ocean (cold water), or about 35°F above the ambient temperature.
2. Tilting of the RTG up to 60 degrees from the vertical does not seriously affect the capability of the convectors to reject the heat produced; therefore, strict verticality will not be a critical requirement in the ocean.
3. The use of a shroud around the convectors to provide a 'chimney' effect is not justified in terms of efficiency; the elimination of the cold water more than offsets any advantage from increased vertical convection.
4. The use of a shroud around the convectors to provide mechanical protection from the projecting convectors and other appurtenances such as electrical connectors which might be placed within the convector circle does not materially inhibit heat transfer, and may be justified on the basis of safety in spite of a small decrease in electrical output.
5. For the flow conditions produced at the power inputs used, the velocities are not high enough to cause washing of the copper surfaces; the use of copper, an optimum material from a heat transfer standpoint, is both justified and highly desirable in this application.

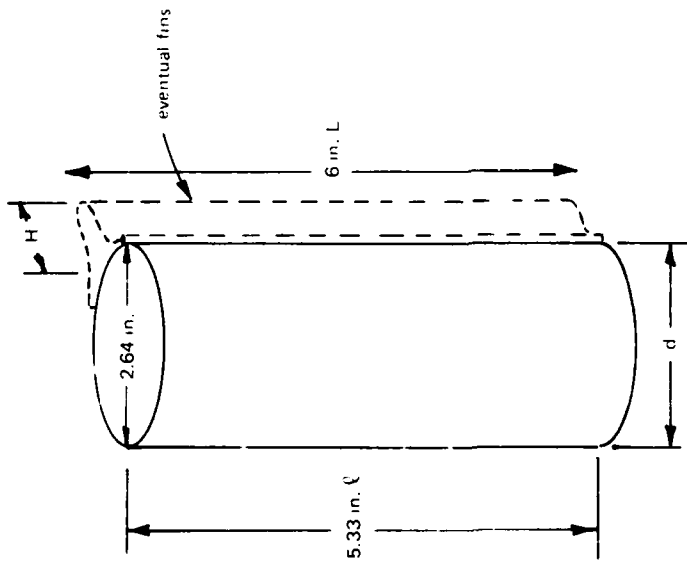


Figure 1. External dimensions of the base area (cold junction) of the thermoelectric units) to be cooled by natural convection to the ocean. Note that fin length, L , is taken slightly longer than the thermoelectric unit length, ℓ (6 inches versus 5.33 inches).

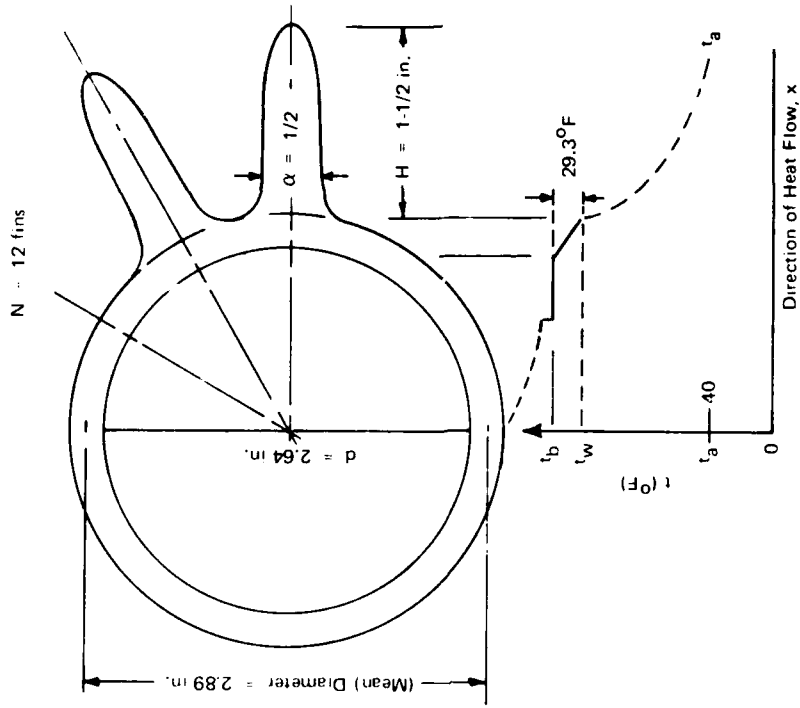


Figure 2. Schematic of proposed fin cross section and temperature drop, if the fins are made of material with $K = 200$, e.g., 70-30 Cu-Ni. The 12-fin system would have an area ratio of 3.85 times the base cylinder, Figure 1.

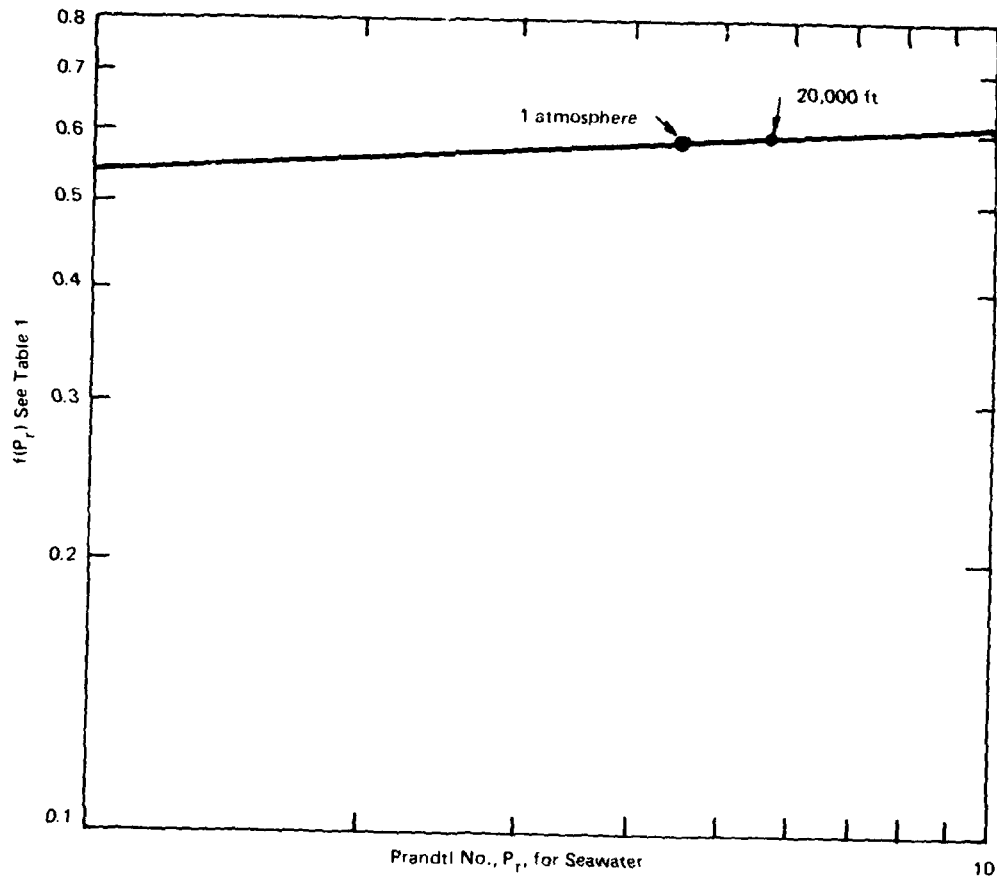


Figure 3. Variation in $f(P_r)$ as P_r varies (in this case by depth and temperature change in the deep ocean).

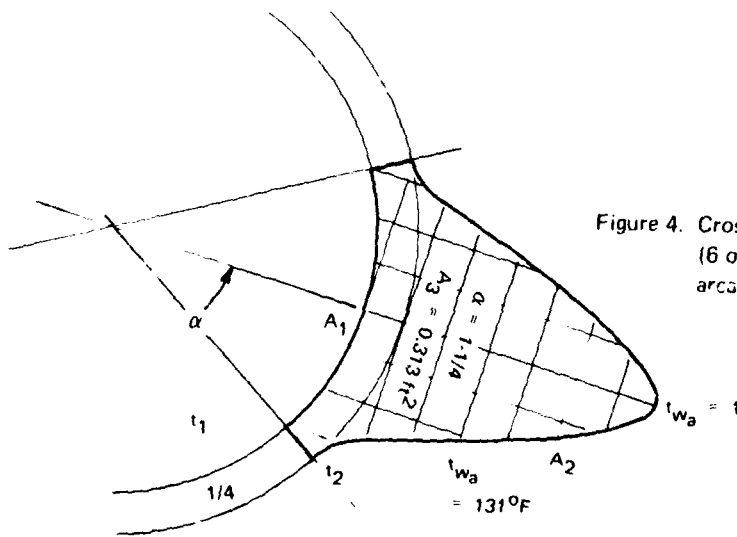


Figure 4. Cross section of a stubby fin (6 on each module) with an arc ratio, R_f , of 2.54.

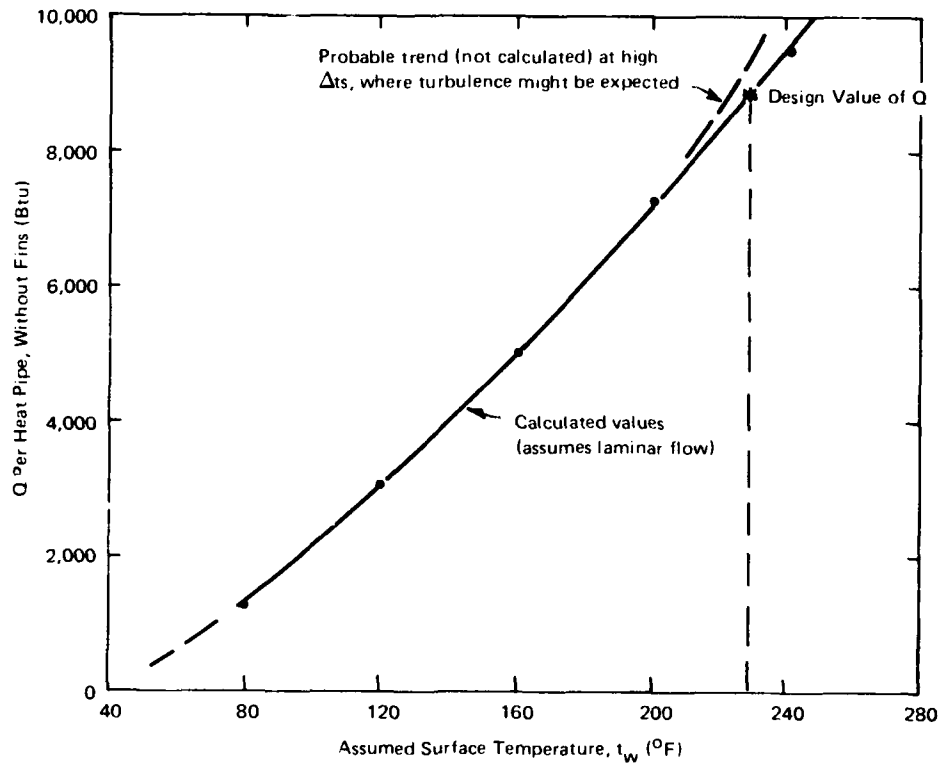


Figure 5. Heat transferred from bare cylinder as a function of surface temperature.

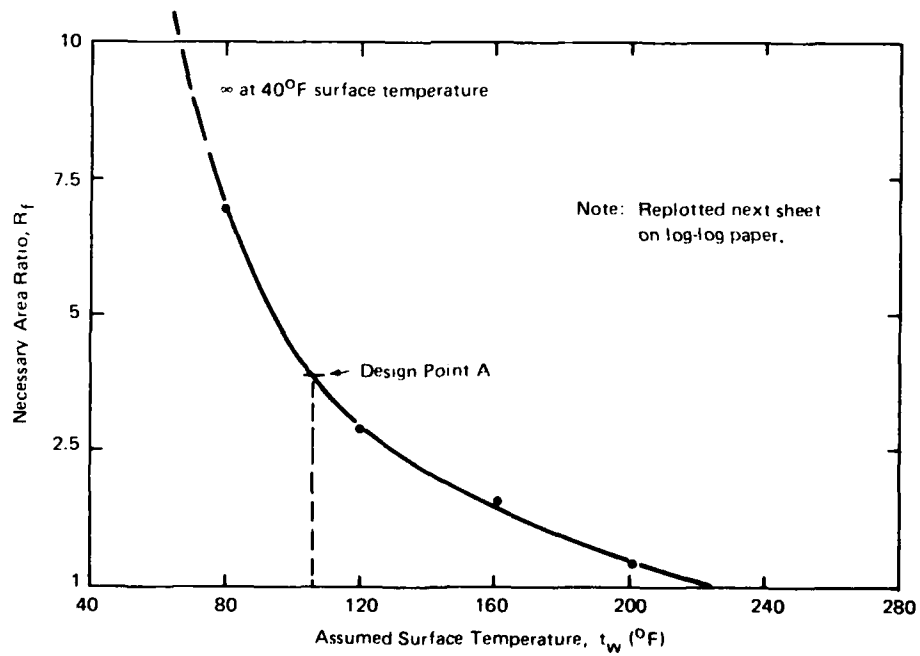


Figure 6. Area ratio necessary to attain desired base surface temperature.

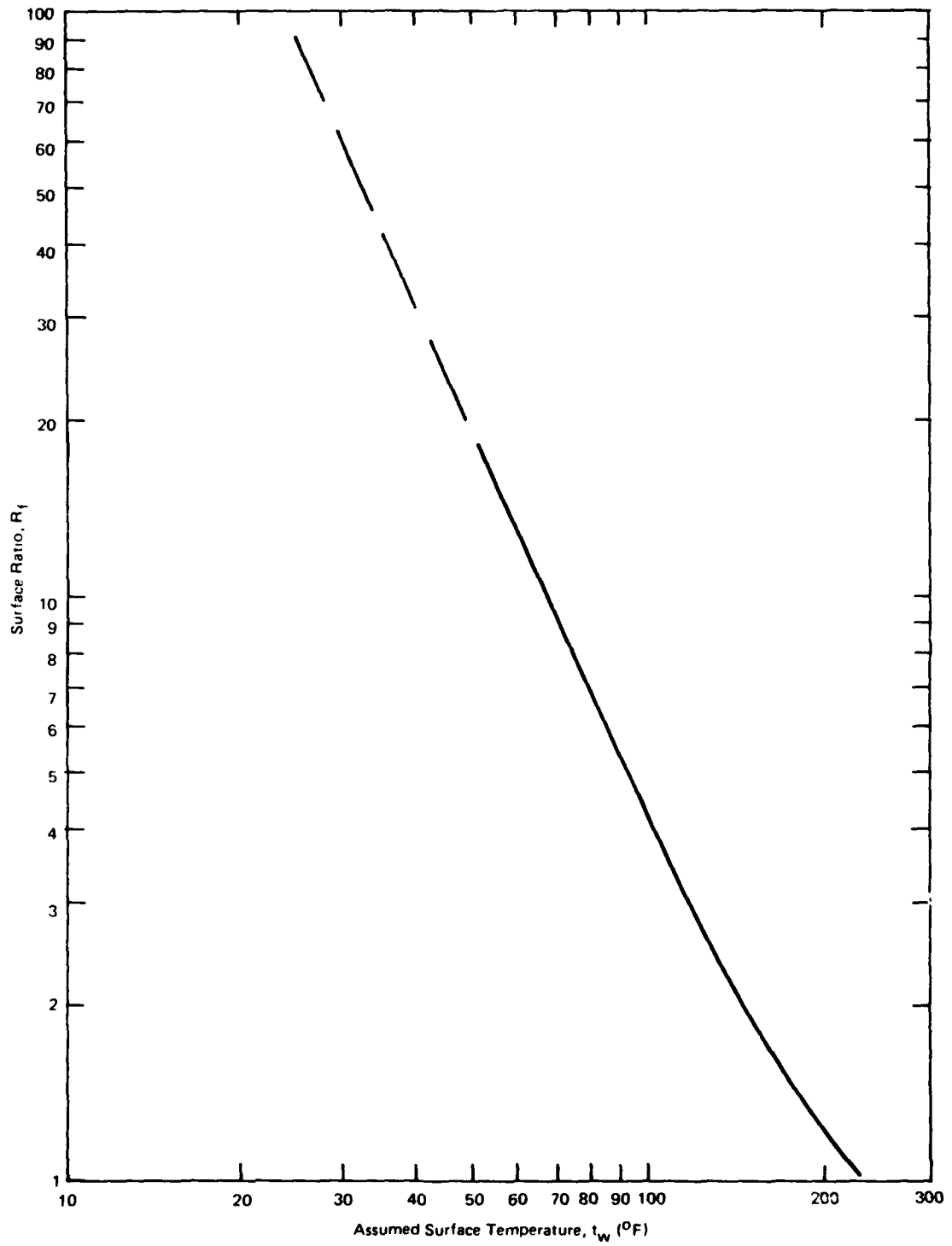


Figure 7. Data for Figure 6 plotted on log-log coordinates showing extrapolation to very low surface temperatures.

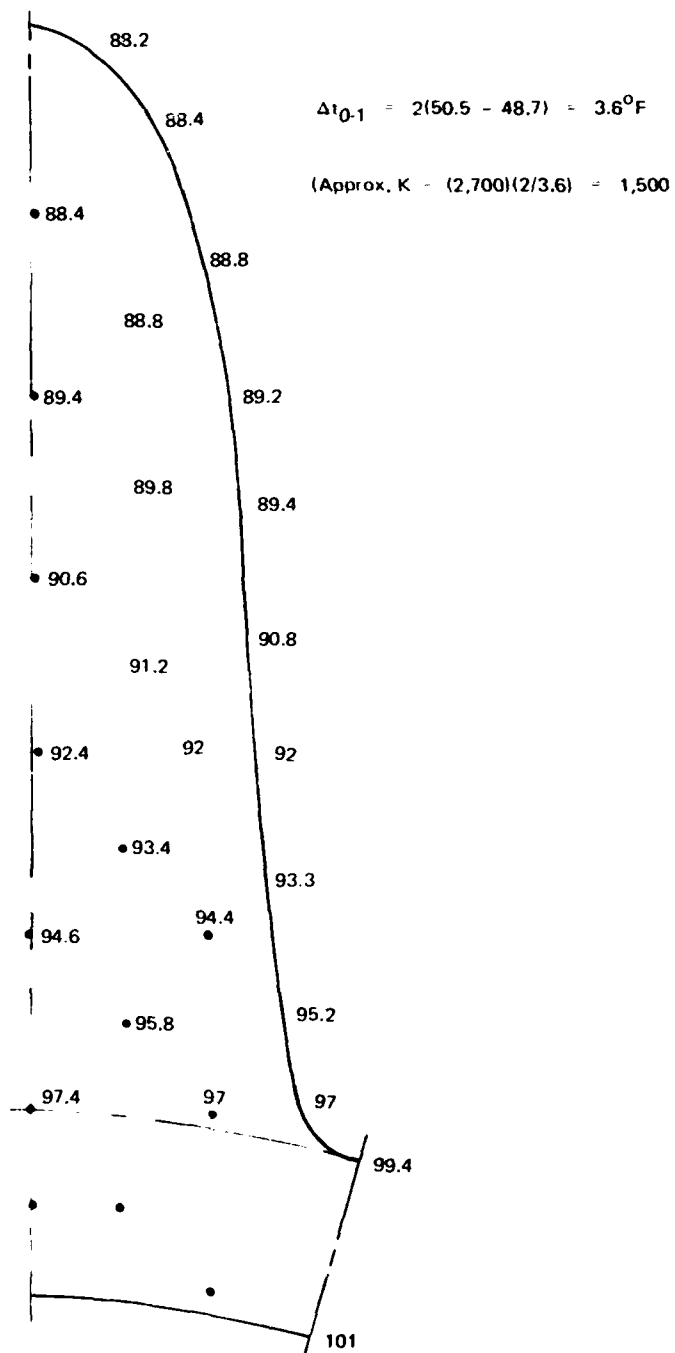


Figure 8. Representative results from analog computer. Values shown would be for metal with conductivity of aluminum.

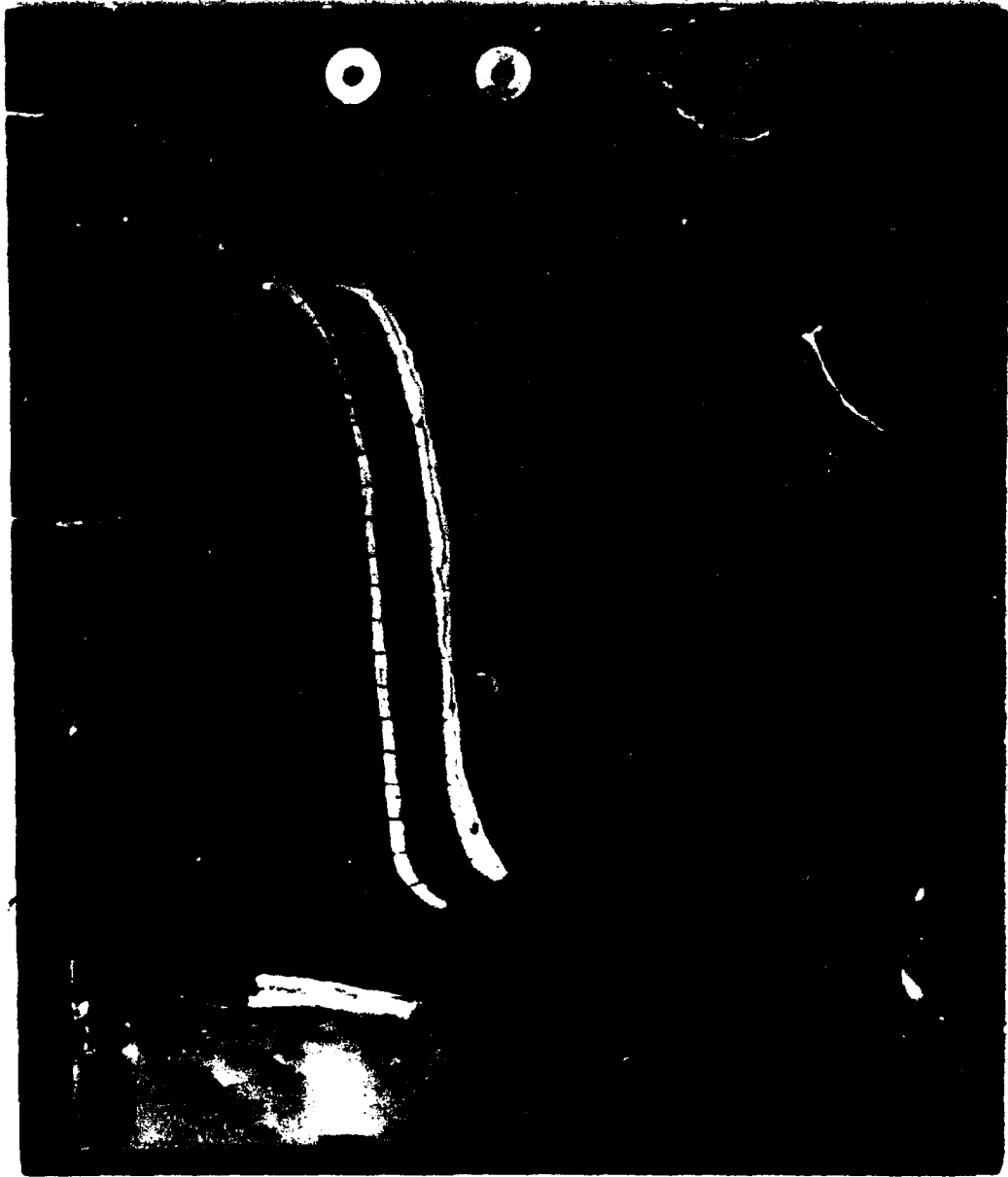


Figure 9. Actual high-resistance surface analog computer with connector wires.

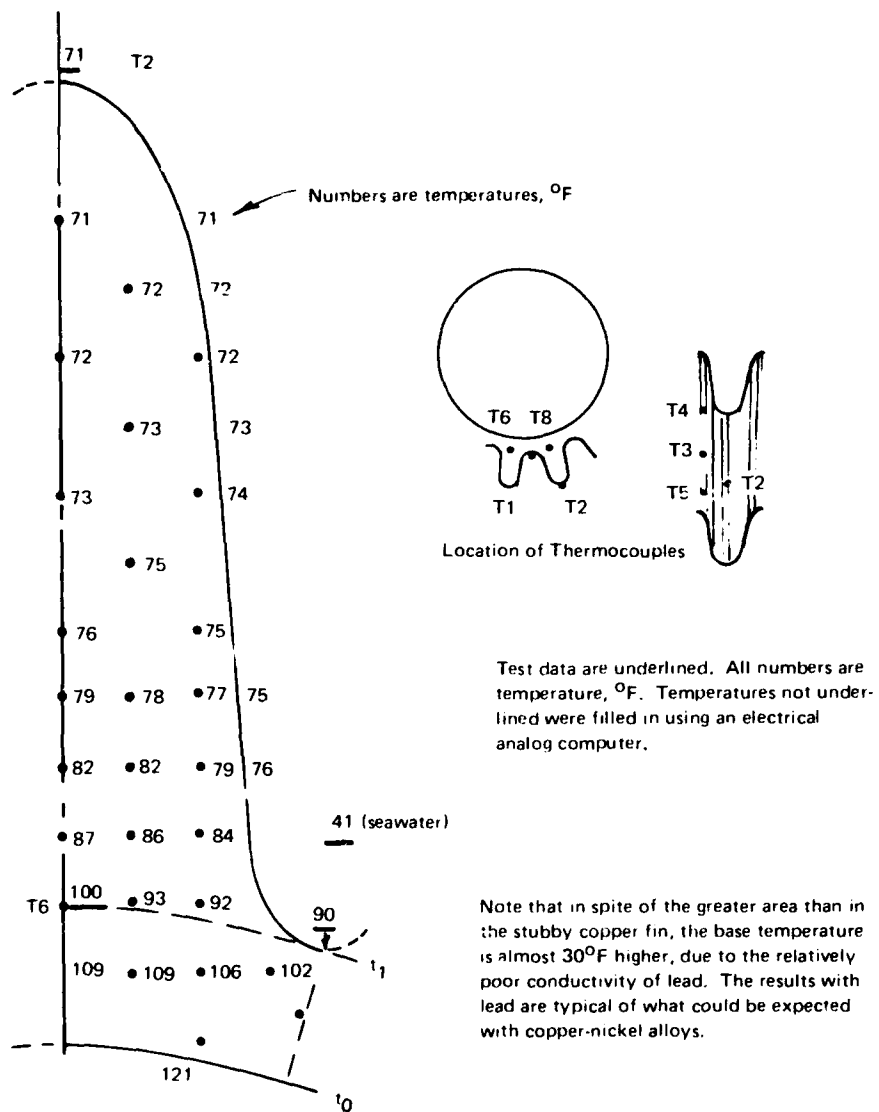
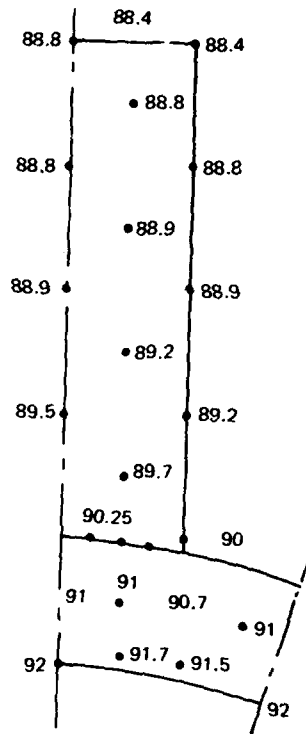


Figure 10(a). Computer output for fins made of lead. Underlined values are experimental, and computer was used to fill in the field.



Four times full size
 Water temperature, 40°F
 Temperature profile obtained by electrical
 analog computer, with temperature drop
 based on the thermal conductivity of
 copper and estimated film transfer
 coefficients, verified in previous
 experiments.

All numbers are temperature, °F.

Note: The computation method requires
 certain assumptions which may change the
 actual values up or down by 1 to 2 degrees;
 the fractional temperatures would not be
 justified on that basis. However, the method
 does provide accuracy of the order indicated
 in establishing temperature gradients.

Figure 10(b). Comparable computer output for stubby copper fins used in the
 12-module experiment. All values shown are calculated.



Figure 11. Full-scale 12-module heat transfer experiment, showing upper ends of heat pipes, with one finned module in place.

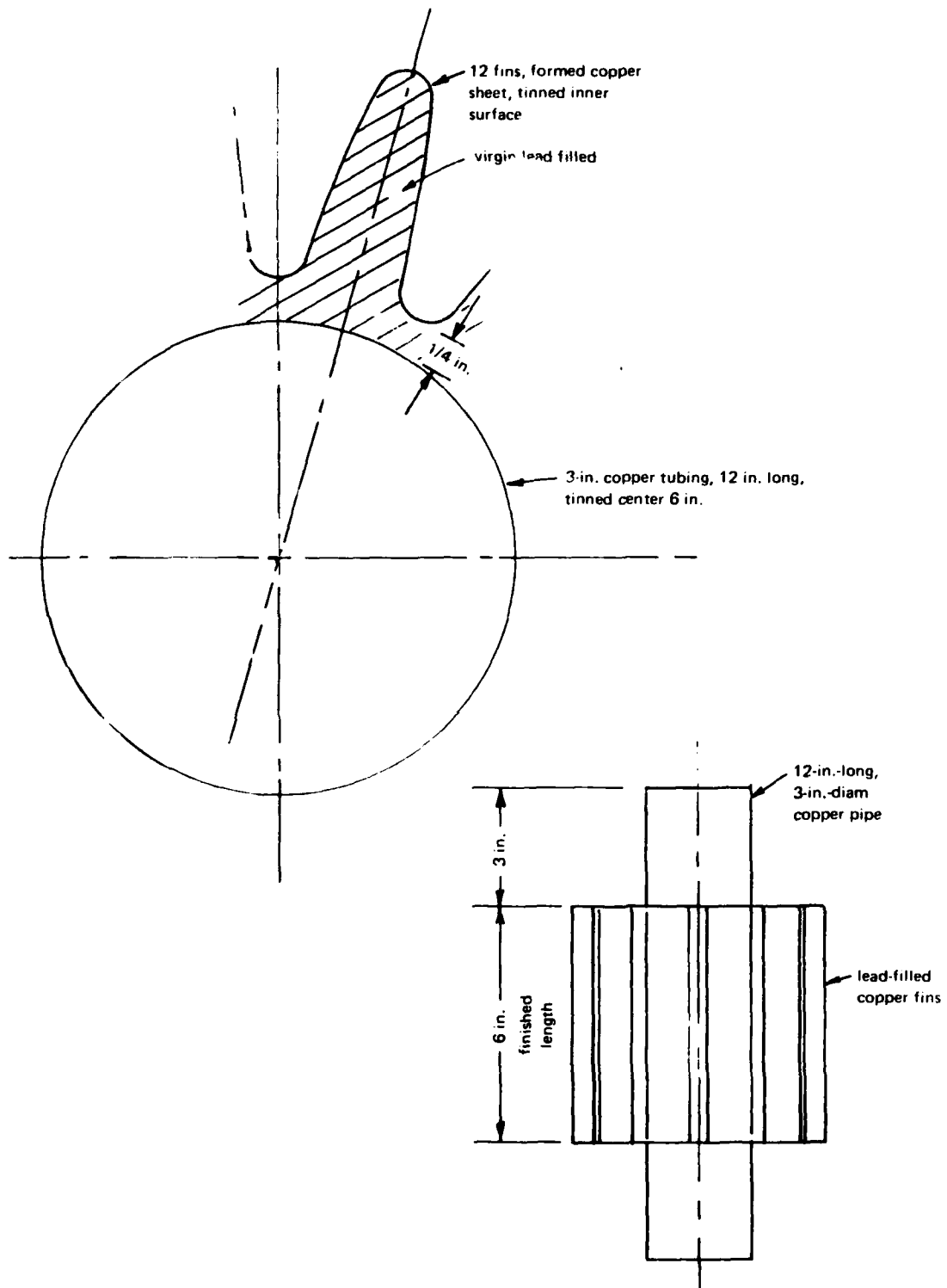


Figure 12. Details of construction of lead-filled exploratory module.

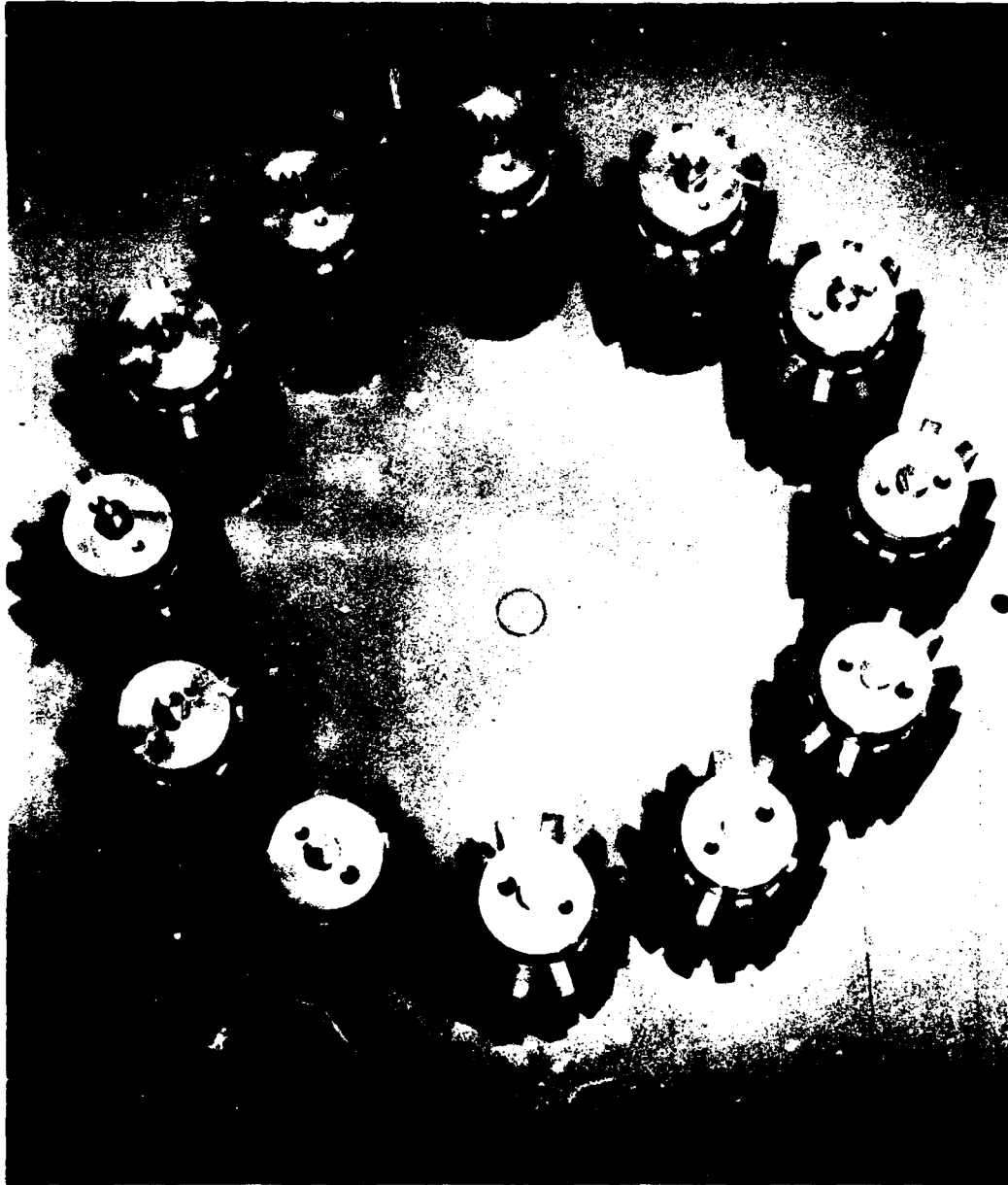


Figure 13. View from above showing 12 heat transfer modules before instrumentation.

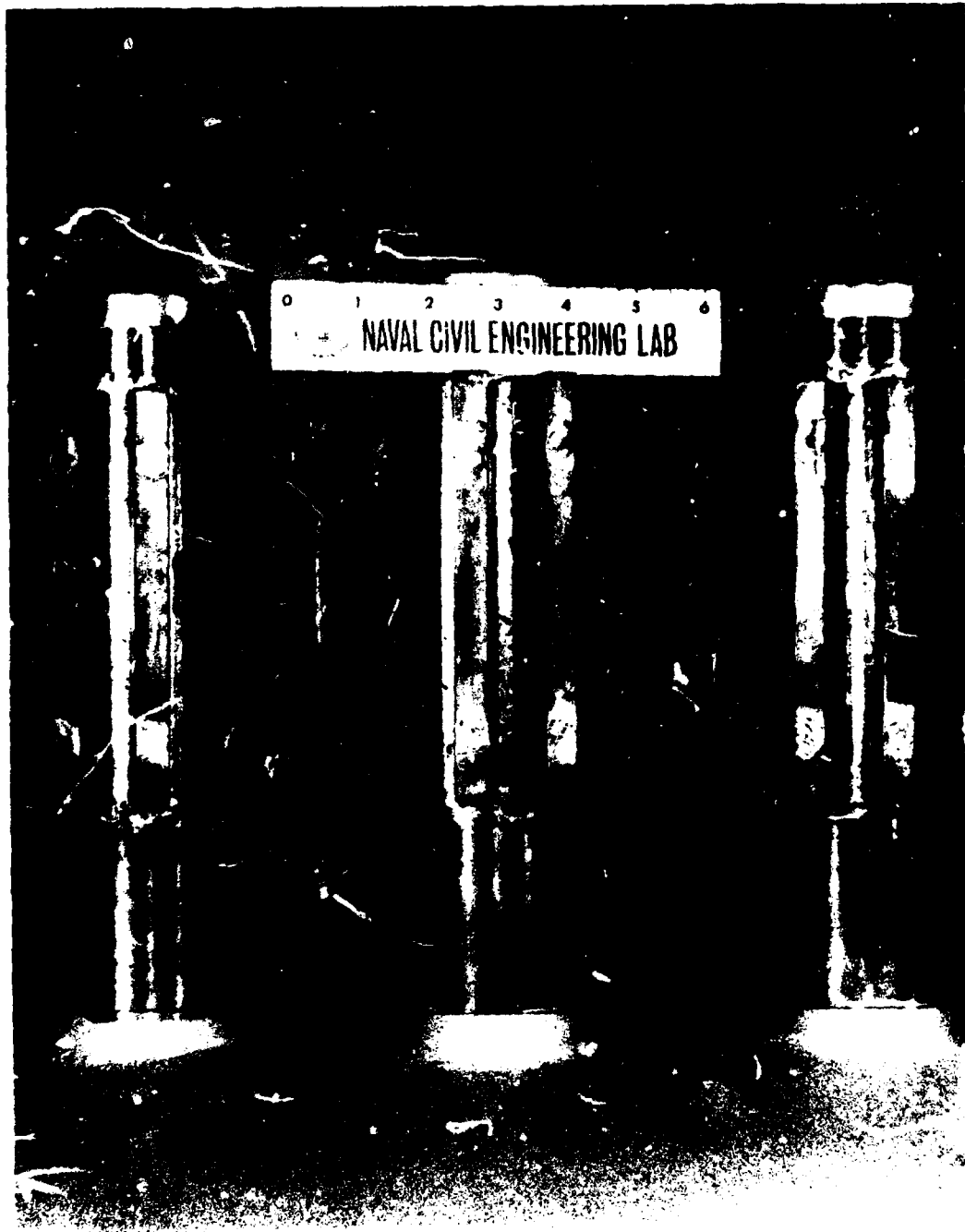


Figure 15. Close-up of finned modules showing close packing which limited length of fins.

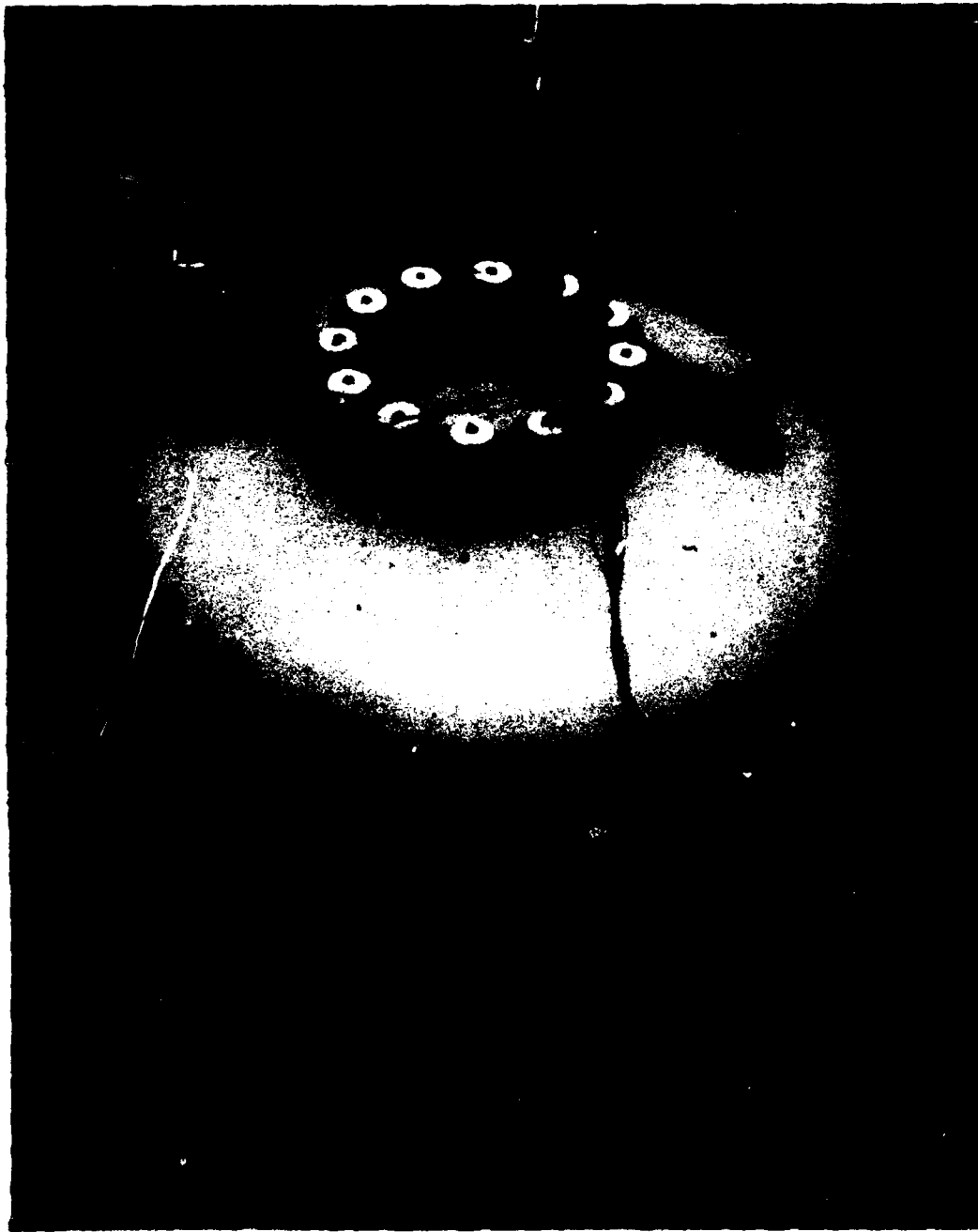
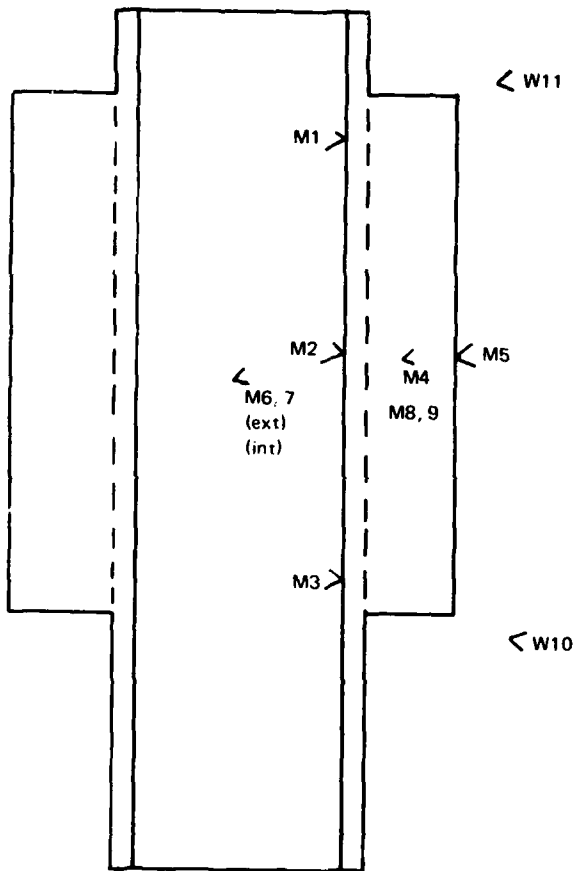
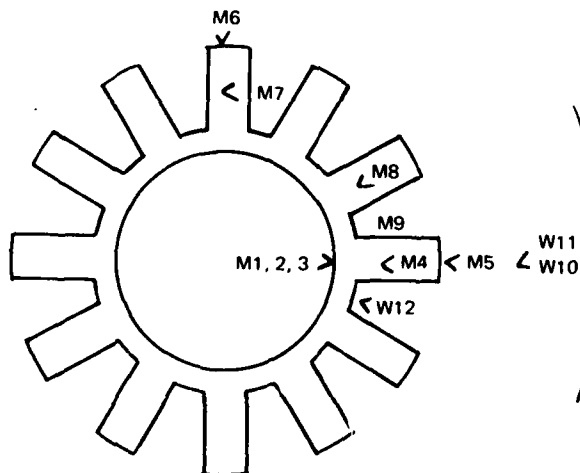


Figure 16. Full-scale 12-module experiment in NCEL saltwater test tank, showing instrument leads and electrical power cable.

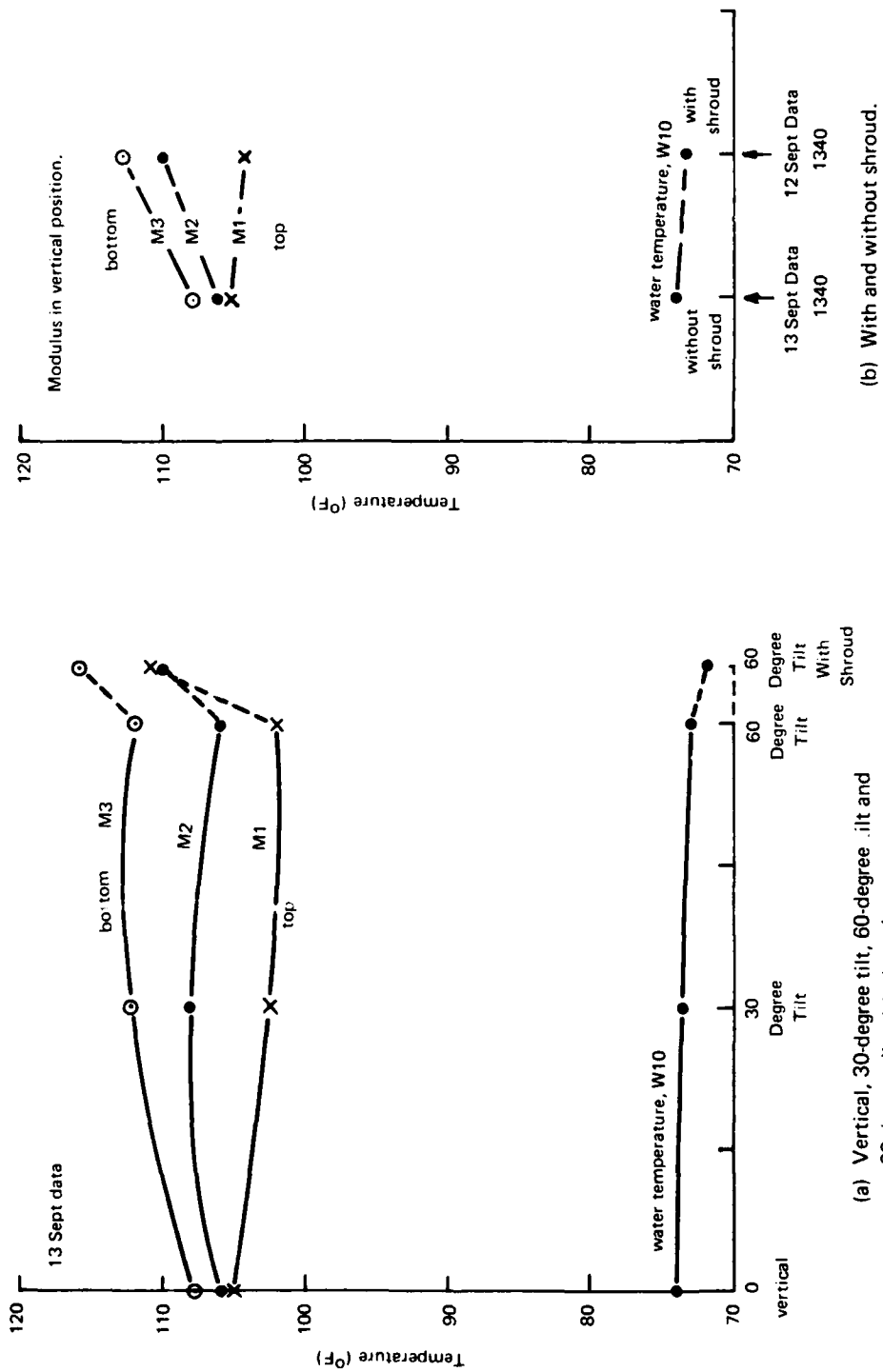


- Notes:
- (1) $\langle M_i, \langle W_i$ indicate positioning of and numbering of thermocouples in metal and water, respectively.
 - (2) All thermocouples to be of nylon insulated, copper constantan, 24 gage, installed to minimize distortion of temperature field or water flow. Wire pairs will be used in water, but single constantan wire peened into copper for all metal temperatures, with common copper return.
 - (3) Readings to be manually recorded, taken on direct reading potentiometer.
 - (4) Complete instrumentation as shown will be applied to one module, with similar critical measurements on adjacent module for comparison.
 - (5) Mid-fin measurements, similar to $\langle M_4$ will be made on one interior fin of every other (six modules total) module, for comparison.
 - (6) Distances of and position of thermocouples in water may be adjusted following first trial tests to insure meaningful readings.



Note: Temperatures indicated in Table 8 are at locations in an adjacent module, similar to M4-M9.

Figure 17. Schematic of copper module showing thermocouple locations.



(a) Vertical, 30-degree tilt, 60-degree tilt and 60-degree tilt with shroud. (b) With and without shroud.

Figure 18. Effect of tilt and shroud on critical metal temperatures (32-kw power input).

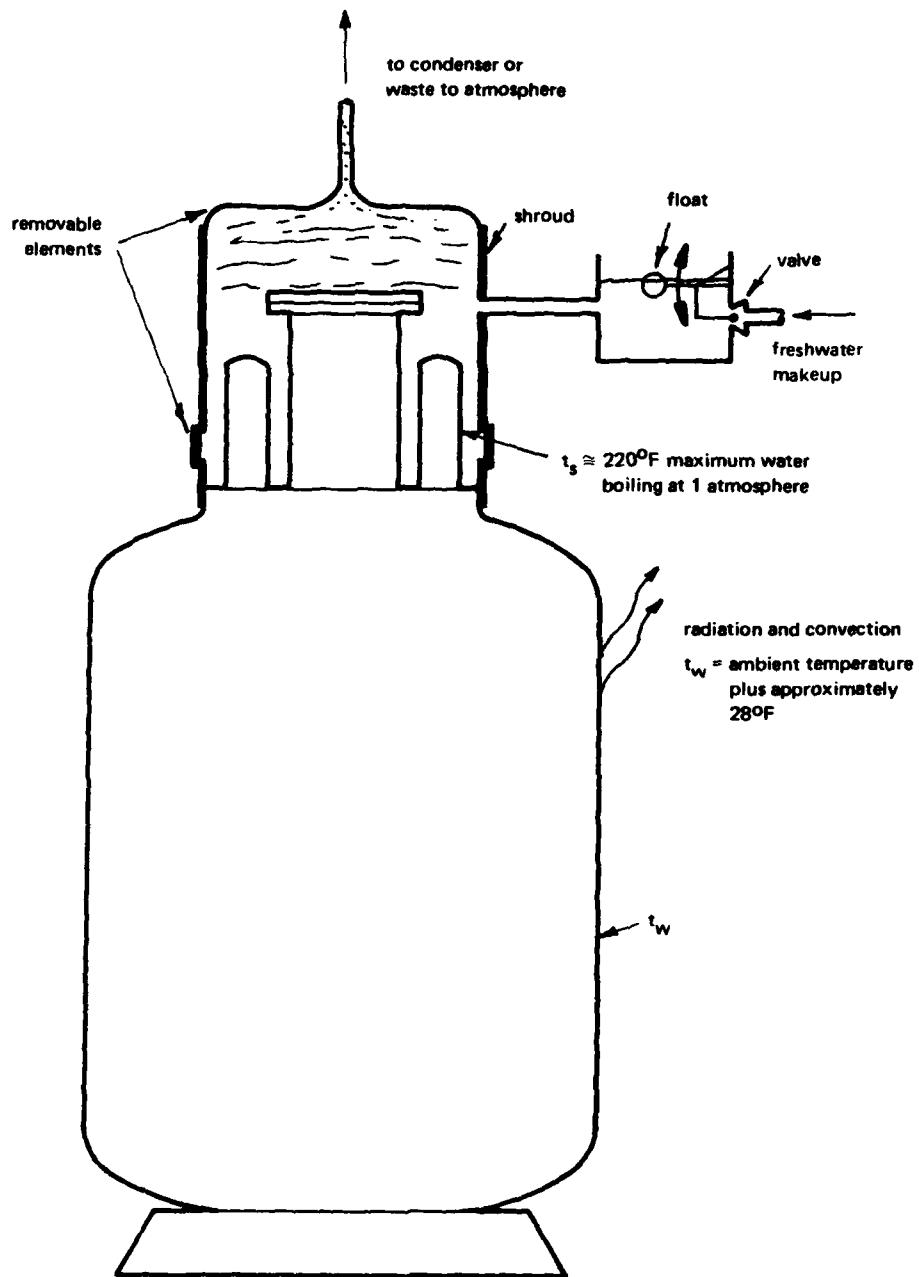


Figure 19. Simplest arrangement for cooling heat pipes during storage or shipment where water supply is limited, as on trains. System requires makeup of about 3 gallons of water an hour.

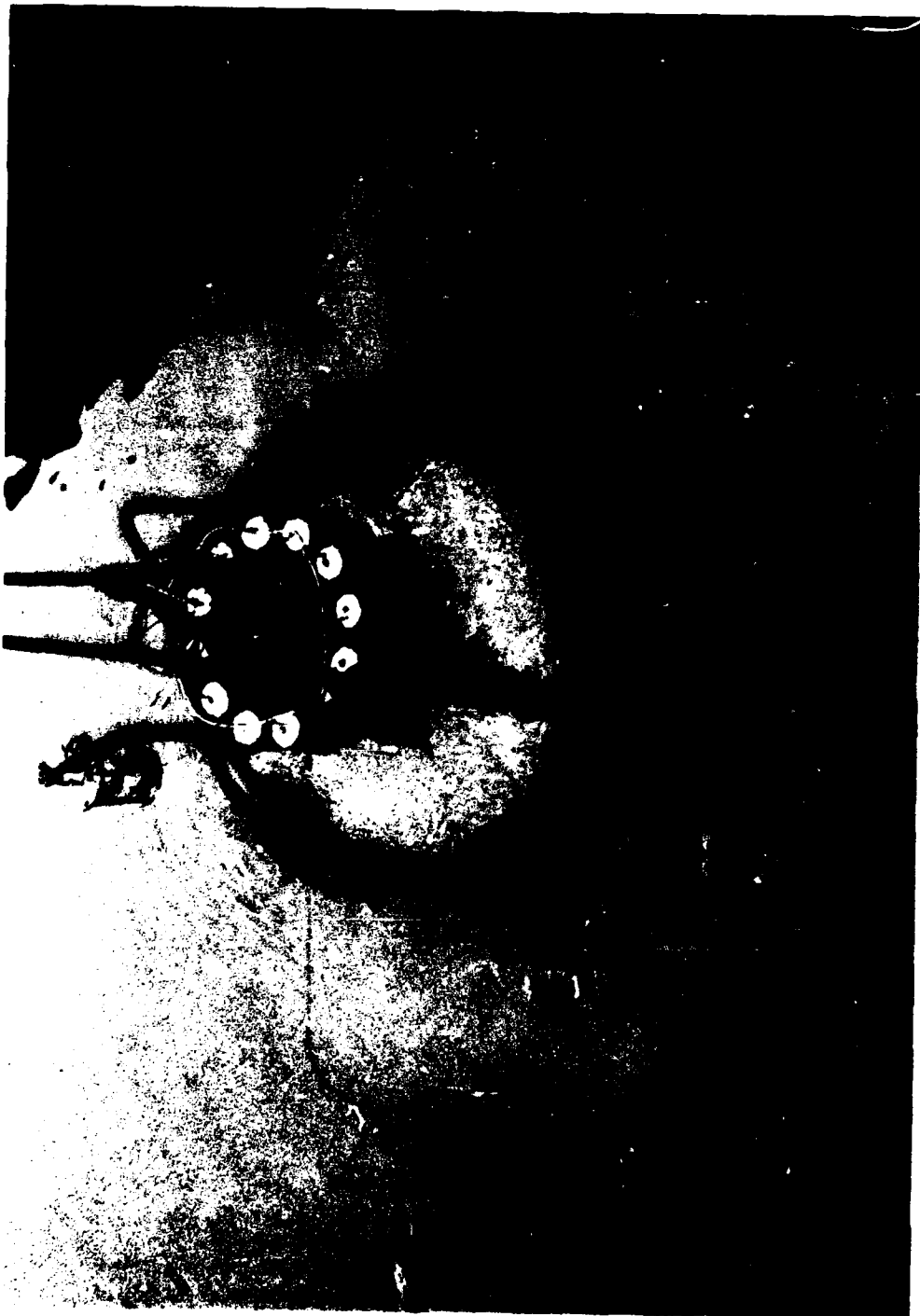


Figure 20. RTG as it emerged from Port Hueneme Harbor after 1-month immersion, 28-kw nominal heat dissipation.

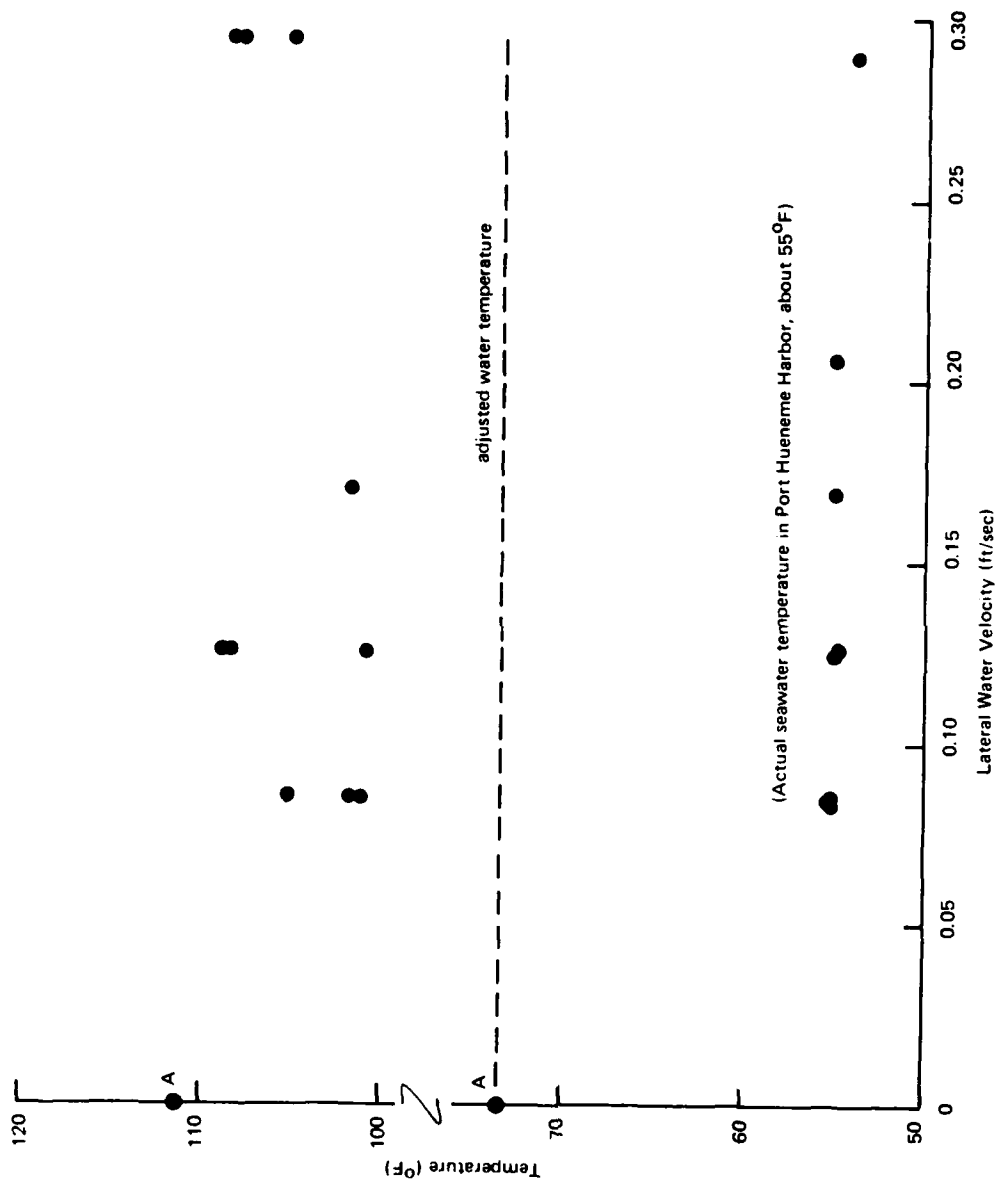


Figure 21. Random plot of average of the three internal metal temperatures as a function of water velocity, adjusted as if the water was the same as the temperature in tank, Points A. Actual seawater temperature in Port Hueneme Harbor, about 55°F.



Figure 22. Closeup of RTG heat transfer modules immediately after removal from Port Hueneme Harbor, 30 day immersion.



Figure 23. RTG upon removal from 30 day immersion, Port Hueneme Harbor, showing non-adherent scum on partially rusty simulated hull.

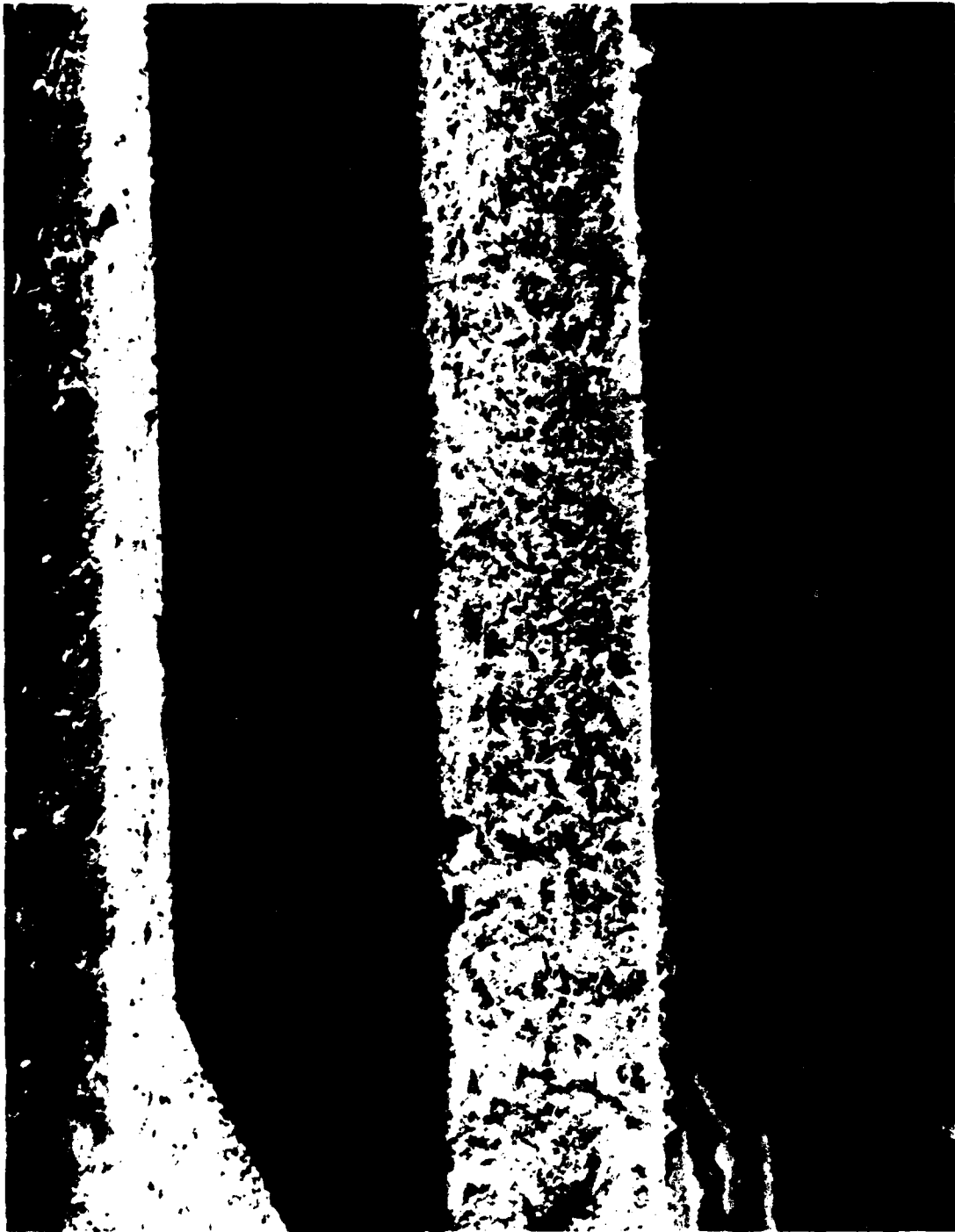


Figure 24. Closeup of RTG heat transfer module fins, following drying, showing early indication of marine growth.

Table 1. Comparative Heat Transfer Parameters in Shallow and Deep Seawater

Parameter	Shallow Water (1 Atm)	20,000-Foot Depth in Ocean
q_r	1.08×10^9	1.235×10^9
P_r	4.5	5.68
R_a	48.6×10^8	70×10^8
$R_a^{1/2}$	2.64×10^2	2.84×10^2
$f(P_r)$	0.58	0.6
N_u^* (mean)	$(0.58)(2.64 \times 10^2) = 1.53 \times 10^2$	$(0.6)(2.89 \times 10^2) = 1.73 \times 10^2$
h_{mean}	$(1.53 \times 10^2)(0.358) = 110$	$(1.73 \times 10^2)(0.35) = 121$

* For shallow water, $N_{u(\text{mean})} = f(P_r)(R_a)^{1/2}$; for deep water, Equation 3 is used.

Table 2. Calculating the Effects of Δt in Shallow Seawater Tests (Independent variable; surface temperature, t_w)

Assumed Surface Temperature, t_w ($^{\circ}\text{F}$)	Δt ($^{\circ}\text{F}$)	$\Delta t_w^{1/2}$	h_{mean}^a	Q/W.O. ^b Fins (Base area of fin)	Fin Area Ratio, R_f , to Reject 8,850 Btu ^c
160	120	3.31	110	5,000	1.76
80	40	2.52	84	1,270	6.95
120	80	2.99	100	3,020	2.92
200	160	3.55	118	7,200	1.22
240 ^d	200	3.76	125	9,450	0.93

^a Based on Approximation

$$h_{\text{mean}_{t_w}} = h_{160} \left(\frac{\Delta t_w}{\Delta t_{160}} \right)^{1/4} = 110 \left(\frac{\Delta t}{3.31} \right);$$

e.g., for $t_w = 80$, $h_{80} = (110) \left(\frac{2.52}{3.31} \right) = 84$

^b Based on $Q = h_m A \Delta t$, where $A = 0.378$.

^c R_f is defined here as surface area ratio of a particular fin system to a plain cylinder of same root diameter, with average surface temperature as shown.

^d Valid approximation at depth in ocean. In shallow water, boiling would keep t_w below about 216°F .

Table 3. Thermal Conductivities of Some Potential Building Materials

Metal	Thermal Conductivity, k [(Btu/(hr)(ft ²)(°F/in.))]
Silver	2,900 ^a
Copper	2,700
Aluminum alloys	1,500 ^b
Magnesium alloy	360 ^c
90-10 Copper-nickel	310
70-30 Copper-nickel	200
Lead, pure	240
Monel	174
Stainless steels	90 to 180
Hastelloy (d)	145
Titanium, pure	118
Typical alloy	60

^a Shown for comparison; has highest value of any known metal.

^b Maximum.

^c Typical.

Table 4. Tabulation of 5 April 1973 Test Temperatures

Time	Temperature (°F) for Locations - ^a									Remarks
	T1	T2	T3	T4	T5	T6	T7	T8	T9	
0940	44	47	40	38.5	38.5	53	50	51		Start vertical; three bags of ice; water temperature = 57°F
0940	90	68	72	61	54	102	166	98	45.5	Power off
0950	90	68	72	61	54	102	166	98	45.5	Power on for 10 min.
1000	87	66	69	61	51	97	163	95.5	43	
1010	90	63.5	67	58	48	98	159	94	36	
1020	94	64	69	62	53	101	158	94	33	
1030	94	71	69	63	54	100	158	94	34	
1040	93	67	70	64	54	102.5	158	94	33	
1050	96	71	74	70	55	104	153	106	37	
1100	90	71	71	75	55	106	158	100	41	Readings shown in Figure 10 (a)
1110										No readings; flipped to 30°
1120	93	70	70	70.5	60	112	157	103	46	

continued

Table 4. (Continued)

Time	Temperature (°F) for Locations - ^a									Remarks	
	T1	T2	T3	T4	T5	T6	T7	T8	T9		
1140	98.7	75	75	79.5	64	119	161	107	52	Tipped 60 degrees left unattended for 20 min.	
1150	100	75	75	81	64	119	160	106	54		
1200	101	77.5	77.5	84	65	120	160	108	56		
1210											
1230	103	66	67	75	57	118	163	108	44		
1240	106	69.5	70	79	60	113	162	106	44		
1250	107	71	71	81	62	119	162	108	44		
1300	107	73	73	83.5	63	124	162	110	45.5		
1310											Tipped back to vertical
1330	119	96	98	98	92	140	173	125.5	58		
1340	122	93	97	100	90	136	172	124	60		
1350	122	94	97	101	90	138	172	124	61		
1400	135	107	110	115	103	149	184	138	76		Power off

^a See Figure 10 (a) for location of thermocouples.

Table 5. Tabulation of 4 April 1973 Test Temperatures

Time	(Single module; 3.1-KW power input)										Remarks
	Temperature (°F) for Locations - ^a										
	T1	T2	T3	T4	T5	T6	T7	T8	T9		
0940	44	48	40	38.5	38.5	38.5	53	50	51		Start vertical; three bags of ice, water temperature = 51°F. Power off. No readings; tilted 30 degrees.
0950	90	68	72	61	54	102	166	98	45.5		
1000	87	66	69	61	51	97	163	95.5	43		
1010	90	63.5	67	58	48	98	159	94	36		
1020	94	64	69	62	53	101	158	94	33		
1030	94	71	69	63	54	100	158	94	34		
1040	93	67	70	64	54	102.5	158	94	33		
1050	96	71	74	70	55	104	158	96	37		
1100	90	71	75	75	55	106	158	100	41		
1110											
1120	93	70	70	70.5	60	112	157	103	46		

continued

Table 5. (Continued)

Time	Temperature (°F) for Locations - ^a										Remarks
	T1	.2	T3	T4	T5	T6	T7	T8	T9		
1140	98.7	75	75	79.5	64	119	161	107	52	Tipped 60° and valve closed.	
1150	100	75	75	81	64	119	160	106	54		
1200	101	77.5	77.5	84	65	120	160	108	56		
1210											
1230	103	66	67	75	57	118	163	108	44	Tipped back to vertical.	
1240	106	69.5	70	79	60	113	162	106	44		
1250	107	71	71	81	62	119	162	108	44		
1300	107	73	73	83.5	63	124	162	110	45.5		
1310										All ice gone, water getting warm. Power off.	
1330	119	96	98	98	92	140	173	125.5	58		
1340	122	93	97	100	90	136	172	124	60		
1350	122	94	97	101	90	138	172	124	61		
1400	135	107	110	115	103	149	184	138	76		

^a See Figure 10 (a) for thermocouple locations.

Table 6. Comparison of Metal Temperature Changes With Water Temperature Change for a Single Vertical Lead-Finned Module

(3-KW power input)			
Thermocouple Location ^a	Temperature (°F) at		Temperature Difference (°F)
	1400 Hr	1100 Hr	
T1	135	90	45
T2	107	71	36
T3	110	75	45
T4	115	75	40
T5	103	55	48
T6	149	106	43
T7	184	158	46
T8	138	100	38
T9 (water)	76	41	35

^a See Figure 10 (a) for location of thermocouples.

Table 7. Tabulation of 13 August 1973
 Test Temperatures For Full-
 Scale, 12-Module Heat Transfer
 Unit

(60,000-gallon seawater tank; 28-KW power input; 1130-hr readings)	
Thermocouple Number	Temperature (°F)
M1	84.7
M2	92.2
M3	90.9
M4	85.8
M5	86.1
M6	85.1
M7	86.7
M8	86.7
M9	86.7
W10	70.3
W11	70.3
W12	71.7
M13 ^b	105
M14	101.3
M15	94.9
M16	107
M17	71.7
W18	70

^a See Figure 17 for thermocouple locations.

^b Thermocouples M13-M17 are on adjacent module
 and are similar in location to M4-M9 shown
 in Figure 17.

Table 8. Tabulation of 12 and 13 September 1973 Temperatures for Full-Scale, 12-Module Heat Transfer Unit in 60,000-gallon NCEL Tank, Seawater

(60,000-gallon seawater tank; 32-KW power input)																			
Time	Temperature (°F) for Locations - ^a																	Remarks	
	M1	M2	M3	M4	M5	M6	M7	M8	M9	W10	W11	W12	M13	M14	M15	M16	M17		M18
1345	103.1	110	113	97.8	101.3	97.2	100	100	100	733	70	71.4	103	101	101.3	101	101.6	70.3	Unit Vertical
1340 ^b	105.4	106.1	108	103	100.3	102	99.5	103	100.8	74	68.7	73	101	104	104	105	97.3	70	Unit Vertical
1350	103	108	112.3	105	105	104.3	104	106.5	104.8	73.5	70	71.8	99	101	104	102	100.5	70.2	Unit tilted 30 degrees
1-00	102.2	105.5	112	105.2	103.2	105.1	104.5	107	105	73	72.1	74.8	97.5	101.5	102.8	98.2	102	70	Unit tilted 60 degrees
	109.1	110.1	116	108.8	108	108	108.9	112.2	109.5	72	70.70	70.70	106	106	108	107.1	88	89.7	Unit with Shroud

^a See Figure 17 for location of thermocouples.

^b Compose with Table 7 readings.

Table 9. Tabulation of Test Temperatures in Huenehme Harbor

(28-KW power input)

Date	Lateral Tidal Current (ft/sec)	Temperatures (°F) for Locations ^a																	
		1	2	3	4	5	6	7	8	9	10	11	12	13	14	15	16	17	18 ^b
Huenehme Harbor Test																			
12 Feb 74	0.211	80.5	80.0	80.0	70.5	72.0	71.0	74.5	71.5	73.0	58.5	58.0	57.7	73.0	73.6	74.0	Open	62.0	55.0
13 Feb 74	0.127	80.0	80.1	79.8	74.0	72.0	70.7	73.0	71.0	72.1	61.0	60.3	59.0	76.0	74.1	73.8	Open	74.0	55.0
14 Feb 74	0.085	82.7	82.3	82.4	75.0	74.6	74.7	76.6	76.6	77.1	59.1	58.5	56.3	78.3	78.7	79.1	Open	78.0	55.0
15 Feb 74	0.085	82.9	82.5	82.5	75.1	74.7	74.8	77.9	76.7	77.1	59.0	58.7	56.4	78.5	78.9	79.2	Open	78.1	55.0
17 Feb 74	0.127	82.8	82.6	82.6	75.0	44.6	74.7	77.8	76.7	77.1	59.0	58.7	56.4	78.5	78.8	79.1	Open	78.1	55.0
19 Feb 74	0.169	82.9	82.5	82.5	75.0	74.6	74.8	77.8	76.7	77.1	59.0	58.7	56.4	78.4	78.9	79.1	Open	78.0	55.0
6 Mar 74	0.085	86.1	86.7	82.0	81.1	82.2	79.5	81.0	79.0	81.2	58.2	58.1	7.0	78.0	Open	78.0	Open	Open	54.0
8 Mar 74	0.294	79.1	79.2	79.3	71.0	70.8	69.4	68.5	68.9	71.4	57.0	56.0	56.8	76.1	Open	68.5	Open	Open	54.0
15 Mar 74	0.294	89.0	90.8	90.8	82.0	80.3	80.3	80.7	81.0	84.0	61.0	60.9	60.0	87.0	Open	89.5	Open	Open	56.0
In-Tank Test ^c																			
10 Aug 73	0	104.2	117.4	112.0	103.0	103.0	101.0	104.2	104.2	105.0	73.7	73.3	76.2	102.1	96.4	94.0	102.4	74.1	73.3

^a See Figure 17 for thermocouple locations.

^b In water.

^c For comparison.

Appendix A

METAL SELECTION FOR NATURAL CONVECTORS IN THE OCEAN

Pure copper is not often used in direct contact with seawater in heat transfer devices, so its selection here should be explained. For hundreds of years, it has been recognized that of all the known metals and finishes, copper is the optimum for inhibiting marine growth. A frequently quoted rule of thumb has been that copper-bearing alloys typically are useful in inhibiting marine growth in proportion to the percent of copper present. The sheathing of wood sailing ships with copper to prevent attack is further justification for this observation.

However, the usual application for nonferrous materials in industrial heat transfer has been condenser tubes--for which copper without alloy is inadequate. This is because of the high velocities required in condenser tubes to give the good heat transfer necessary to make condensers of a reasonable size and cost. As a rule of thumb, there is no apparent corrosion of copper at velocities below about 4 to 6 ft/sec, depending upon tube size, no matter how long it is immersed or exposed. At significantly higher velocities, the surface 'washes'; a continually new layer of copper is exposed and removal rates in excess of 0.002 inch per year from this velocity effect are typical.

For the heavy fins that are optimal in high capacity convectors, (for reasons given in the design section), such washing rates would not be prohibitive. However, estimates based on Grashoff's number (10^9) might be expected to produce maximum velocities of a few feet per second. From these low velocities and the unconfined nature of the flow, it was quickly determined that copper was the best available material because of its excellent properties in all other respects--corrosion, fouling, and high thermal conductivity. Since no washing of the (slightly oxidized) convectors has been observed to date, the choice appears to be justified insofar as these experiments are concerned. Also, the tests in Port Hueneme Harbor provided further evidence on this as well as the all-important consideration not within the scope of the laboratory-type experiments--fouling in the actual ocean environment.

Appendix B

30-DAY IMMERSION TESTS IN PORT HUENEME HARBOR

Following completion of the controlled laboratory tests reported in the main body of the report, it was decided to immerse the unit under power in the Port Hueneme Harbor for a month. This additional testing would have several potential benefits: determination of RTG temperature at lower water temperatures than could be readily obtained in the test tank, the incipient formation of biological scum, and the temperature effects of small tidal currents acting across the copper finned heat rejection surfaces.

The instrumentation for these tests was the same as used in the earlier laboratory tank tests, except that the test unit was fitted with a carefully calibrated Savonius Rotor Current Meter at the same level as the heat transfer surfaces, Figure 20. One thermocouple failed (opened) before any readings were taken, but since it was very expensive to remove the unit from the water and replace, the thermocouple was not repaired.*

It was originally planned to set the entire RTG on the bottom on a hardwood pallet; a survey of the proposed area by CEL divers indicated suitable near-level areas. However, early attempts to stabilize the RTG on the bottom showed that the bottom was neither level nor stable within a reasonable distance of the wharf. It was eventually suspended by a heavy synthetic line just off the bottom in about 25 feet of water (Figure 20). The bottom of the RTG was sufficiently close to the harbor bottom to stir up mud upon its retrieval. The heat rejection surfaces were about 19 feet below the water surface at mean tide.

Typical temperatures taken during the 30-day immersion period are shown in Table 9 with varying currents. In the earlier laboratory tests, the power level was varied from the nominal 32 kw by changing the voltage from a portable generator. In these tests, power output was determined by the CEL dock-side voltage, yielding a heat dissipation of approximately 8 kw or about 11% less than the nominal.

In Table 9 the temperatures taken in the harbor, where the experiment was exposed to water some 18°F colder than in the earlier laboratory tank tests, are compared with data taken 10 August 1973 in the tank (last column). All things being equal, it would be expected that typical metal temperatures in the harbor would be about 18°F colder than in the tank due to the colder water. Also, the current effect, while probably slight and variable, should be discernible. To allow direct comparison, the temperature differences are increased by the 18°F water temperature difference, Figure 21.

* It was a surface temperature reading in a partially instrumented module and was not important in the analysis.

In Figure 21 the average of thermocouple readings for the important temperatures measured by 1, 2, and 3 junctions of the thermoelectric units in a complete RTG are plotted against measured velocity, irrespective of the direction of water flow. These are important data points because they provide the design temperature for the cold junctions in the RTG. Point A is the average of the same readings for the August 1973 tank experiments, without flow. The velocities indicated are those at the beginning of a set of readings, but frequently they varied by 100% during the time required to take 18 thermocouple readings of the temperature. The actual variability in average velocities for several minutes before a series of readings would be responsible for the small variations shown. Fluctuations in line voltage would also produce random variations; for the harbor data shown, there was no control of power input, nor was it monitored continuously.

In summary, low velocities of the order of 0.1 to 0.3 ft/sec enhance the heat transfer from a convector in the ocean, but not significantly in terms of overall electrical generation efficiency. The important point is that any change, while transient and unpredictable, will always be conservative in that cold junction temperatures will be depressed and generator efficiency enhanced in the presence of ocean currents.

NOTES ON CORROSION

The experimental work discussed in this report is directed only to the heat transfer, particularly to provide a minimum temperature at the cold junctions of the RTG's thermoelectric units. The planned tests required only short-term, periodic immersion during which no significant corrosion would be expected. Surface treatment of the large steel shell, Figure 13, was entirely cosmetic and did not include extensive precleaning or priming. The ends of the heat pipes, which would have been capped with pure copper for long-term immersion, were capped with a more readily available, less expensive, and more easily machined aluminum alloy. The 30-day immersion tests discussed in this Appendix provided a brief check on the corrosion handbooks. Since aluminum alloys are electrically much more active in seawater than either copper or steel (with E_H^* of -0.80, -0.70, and -0.40 volt, respectively, for aluminum alloy, steel, and copper), the aluminum caps corroded severely. There was some corrosion of the steel adjacent to the copper fins and none of the copper (Figure 22).

Several alternatives, none of which will probably afford complete protection from corrosion for all parts of the RTG, are available in the final RTG design. One solution might be to cover all the RTG surfaces with heavy copper plating, either electrolytic or rolled. Welding would introduce holidays in a rolled plating, so electrolytic plating might be the more acceptable of these approaches. Electroplating the entire

* E_H is the no-current voltage versus a saturated calomel electrode.

RTG hull and the copper heat transfer surfaces with pure iron is a distinct possibility. Electroplating of the copper surfaces with pure iron with a maximum protection of the remainder of the steel with a dense epoxy or similar protective treatment would be relatively inexpensive. Some form of cathodic protection would be desirable. The fact that the RTG will provide a continuous source of DC electrical power suggests consideration of an active impressed current cathodic protection system. Such systems require continuous, active voltage control to ensure protection, and since the RTG will be unavailable for service of such controls, this appears to be an unsatisfactory solution.

NOTES ON MARINE FOULING

It is a useful rule-of-thumb that the effectiveness of anti-fouling surface treatments in seawater is in proportion to their copper content. With pure copper heat transfer surfaces, no fouling would be expected nor was it observed. Neither was it observed on the painted steel parts; it can be assumed that the immersion period was too short.

On the copper and steel surfaces, there was a loose gelatinous scum consisting of microscopic organisms; it is referred to in the literature as the primary film. This film was over the entire hull and was approximately 1/16 inch thick. There was no strongly adhering macroscopic fouling, as for instance, barnacles (Figure 23). This is consistent with what was observed in similar but longer tests by Braun (1965), Figure 24. With slightly warmer surfaces there is apparently an enhancement of marine growth which would eventually cause some increase in the film coefficient of heat transfer and a slight elevation of the surface metal temperatures. The Braun work clearly showed that after perhaps 5 or 6 weeks, a maximum growth would be attained, and no further degradation in heat transfer would be expected. There are no observable inconsistencies in the present work with the earlier, more definitive experimental results as reported by Braun (1965).

LIST OF SYMBOLS

A	Base area (ft ²)
a	Base thickness of fin (ft)
c _p	Specific heat [Btu/(lb)(°F)], at constant pressure
D	Outside diameter of thimble
E _H	No-current voltage compared to saturated calomel electrode
f	Experimental constant
g	Local gravitational constant
H	Radial height of fin
h	Convection film coefficient
K	Thermal conductivity [Btu/(hr)(ft ²)(°F/ft)]
k	Thermal conductivity [Btu/(hr)(ft ²)(°F/in.)]
L	Fin length
ℓ	Length of thermoelectric unit (TE)
N	Number of fins
Nu	Nusselt's number, = hd/K
P	Pressure (psi)
Pr	Prandtl number
Q	Heat transferred (Btu/hr)
Ra	Rayleigh Number = (Pr)(qr) = (C _p μ/K)(L ³ ρ ² β _q Δt/μ ²)
R _f	Surface area ratio of fin system to plain cylinder of same root diameter
S _c	Longitudinal compressive stress (psi)
t _a	Temperature of water (°F)

t_b Temperature of thimble base, Figure 2 ($^{\circ}\text{F}$)
 t_m Temperature of surface thermoelectric unit ($^{\circ}\text{F}$)
 t_w Water temperature
 t_{wa} Ambient water temperature
 x Dimension in direction of heat flow
 β Thermal coefficient of expansion of seawater ($^{\circ}\text{F}^{-1}$)
 Δt Temperature difference, metal surface to water ($^{\circ}\text{F}$)
 μ Viscosity, $\text{lb}/(\text{ft})(\text{hr})$
 ρ Density of seawater (lb/ft^3)